ENVISAT GOMOS Monthly report: June 2006
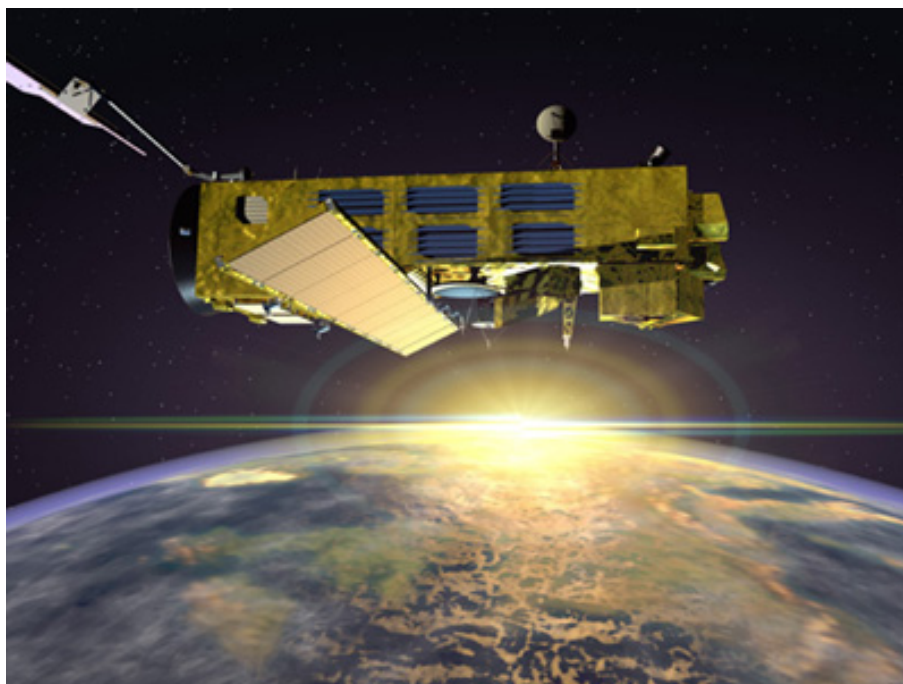
T A B L E   O F   C O N T E N T S

1   INTRODUCTION

The GOMOS monthly report documents the current status and recent changes to the GOMOS instrument, its data processing chain, and its data products.

The Monthly Report (hereafter MR) is composed of analysis results obtained by the Data Processing and Quality Control, combined with inputs received from the different entities working on GOMOS operation, calibration, product validation and data quality. These teams participate in the GOMOS Quality Working Group:

- European Space Agency (ESRIN, ESOC, ESTEC-PLSO)
- DPQC
- ACRI
- Service d'Aeronomie
- Finnish Meteorological Institute
- IASB-Belgian Institute for Space Aeronomy
- Astrium Space
- ECMWF

In addition, the group interfaces with the Atmospheric Chemistry Validation Team.

1.1   Scope

The main objective of the Monthly Report is to give, on a regular basis, the status of GOMOS instrument performance, data acquisition, results of anomaly investigations, calibration activities and validation campaigns. The following six sections compose the MR:

- Summary
- Unavailability
- Instrument Configuration and Performance
- Level 1 Product Quality Monitoring
- Level 2 Product Quality Monitoring
- Validation Activities and Results

1.2   References

[1]   ENVISAT Weekly Mission Operations Report #205, 206#, #207, #208, #209 ENVI-ESOC-OPS-RP-1011-TOS-OF
[2]   ECMWF GOMOS Monthly Reports

1.3   Acronyms and Abbreviations

ACVT   Atmospheric Chemistry Validation Team
ADC   Analogue-to-Digital Converter

ADF	Auxiliary Data File
ADS	Auxiliary Data Server
ANX	Ascending Node Crossing
ARB	Anomaly Review Board
ARF	Archiving Facility (PDS)
CCU	Central Communication Unit
CFS	CCU Flight Software
CNES	Centre National d'Études Spatiales
CTI	Configuration Table Interface / Configurable Transfer Item
CR	Cyclic Report
DC	Dark Charge
DMOP	Detailed Mission Operation Plan
DPM	Detailed Processing Model
DPQC	Data Processing and Quality Control
DS	Data Server
DSA	Dark Sky Area
DSD	Data Set Descriptor
ECMWF	European Centre for Medium Weather Forecast
EQSOL	Equipment Switch Off Line
ESA	European Space Agency
ESL	Expert Support Laboratory
ESRIN	European Space Research Institute
ESTEC	European Space Research & Technology Centre
ESOC	European Space Operations Centre
FCM	Fine Control Mode
FMI	Finnish Meteorological Institute
FOCC	Flight Operations Control Centre (ENVISAT)
FP1	Fast Photometer 1
FP2	Fast Photometer 2
GADS	Global Annotations Data Set
GOMOS	Global Ozone Monitoring by Occultation of Stars
GOPR	Gomos Prototype
GS	Ground Segment
HK	Housekeeping
IASB	Institut d'Aeronomie Spatiale de Belgique
IAT	Interactive Analysis Tool
ICU	Instrument Control Unit
IDL	Interactive Data Language
IECF	Instrument Engineering and Calibration Facilities
IMK	Institute of Meteorology Karlsruhe (Meteorologisch Institut Karlsuhe)
INV	Inventory Facilities (PDS)
IPF	Instrument Processing Facilities (PDS)
JPL	Jet Propulsion Laboratory
LAN	Local Area Network
LMA	Levenberg-Marquardt Algorithm
LPCE	Laboratoire de Physique et Chimie de l'Environnement
LUT	Look Up Table
MCMD	Macro Command

MDE	Mechanism Drive Electronics
MIP	Most Illuminated Pixel
MPH	Main Product Header
MPS	Mission Planning System
MR	Monthly Report
OBDH	On-Board Data Handling
OBT	On Board Time
OCM	Orbit Control Manoeuvre
OOP	Out-of-plane
OP	Operational Phase of ENVISAT
PAC	Processing and Archiving Centre (PDS)
PCF	Product Control Facility
PDCC	Payload Data Control Centre (PDS)
PDHS	Payload Data Handling Station (PDS)
PDHS-E	Payload Data Handling Station – ESRIN
PDHS-K	Payload Data Handling Station – Kiruna
PDS	Payload Data Segment
PEB	Payload Equipment Bay
PLSOL	Payload Switch off Line
PMC	Payload Module Computer
PRNU	Pixel Response Non Uniformity
PSO	On-Orbit Position
QC	Quality Control
QUARC	Quality Analysis and Reporting Computer
QWG	Quality Working Group
RGT	ROP Generation Tool
RIVM	Rijksinstituut voor Volksgezondheid en Milieu
ROP	Reference Operations Plan
RTS	Random Telegraphic Signal
SA	Service d'Aeronomie
SAA	South Atlantic Anomaly
SATU	Star Acquisition and Tracking Unit
SFA	Steering Front Assembly
SFCM	Stellar Fine Control Mode
SFM	Steering Front Mechanism
SM	Service Module
SMNA	Servicio Meteorológico Nacional de Argentina
SODAP	Switch On and Data Acquisition Phase
SPA1	Spectrometer A CCD 1
SPA2	Spectrometer A CCD 2
SPB1	Spectrometer B CCD 1
SPB2	Spectrometer B CCD 2
SPH	Specific Product Header
SQADS	Summary Quality Annotation Data Set
SSP	Sun Shade Position
SZA	Solar Zenith Angle
VCCS	Voice Coil Command Saturation

2   SUMMARY

Operations (section 3.1): During the reporting month the instrument was working well without any unavailability period and without any occurrence of the VCCS anomaly.

There were six synchronous sequences with occultations starting very high above the atmosphere in order to check the behaviour of the SATU abnormal oscillations at those altitude ranges. The ranges used were [280, 5], [200, 5] and [150, 5] km (section 4.1.2).

Data availability (when instrument was in operation): For June the level 0 data availability is a little bit lower that nominal (~97%) due to an unavailability of ARTEMIS satellite with subsequent missing of dumped GOMOS data to ESRIN station. For level 1b the archived products are around 86%. The reason for the low statistics on level 1b products respect to level 0 is that the allocated processing time is lower than the real processing time with the result that the end of the orbit is systematically not processed. Now the problem is known and is pending of resolution (section 3.4).

Pointing performance: the SATU NEA ("Y" axis) has a gradual increase since mid April 2006. This increase is due to fluctuations of the SATU 'Y' data observed at the beginning of the occultations (starting at 130 km that corresponds to an elevation angle of around 65°). Special occultations have been performed starting at 280/250/200 km in order to check at which angle the fluctuations start but surprisingly there are two elevation angle ranges for which the fluctuations appear. Preliminary investigations carried out by the ESL, ESA and industry point to a problem on the SFM (mechanical or electrical) and not to a problem on the SATU itself. Since mid June the increase seems to be stable at around 5.5 micro radians. Future monthly reports will inform on the status of this anomaly which is carefully monitored (section 4.6.1).

Temperatures: The CCD temperatures show the expected global increase due to the radiator ageing. Another expected variation of the temperatures, the seasonal one, with amplitude of around 0.8 degree can also be observed (section 4.3).

Modulation signal: The standard deviation of the modulation signal presents high values during summer time. The South Atlantic Anomaly is now confirmed as the cause of these unexpected peaks. The quality of ESRIN data, in particular over the SAA zone, is impacted but the measure of this impact is under investigation. However, in the second half of October, the peaks are smaller because the DSA zone where the data are taken for this analysis is moving towards the Northern Hemisphere. At the end of October the DSA zone is definitely chosen by the planning system in the Northern Hemisphere (to fill the criteria 'DSA in full dark limb conditions') and the high peaks disappear (section 4.5.2).

Star detection performance: the stars should be detected not far from the SATU center, that is, pixel number 145 in elevation and number 205 in azimuth. It has been observed that the azimuth MIP was within the threshold since September 2002 until the occurrence of the VCCS anomaly on January 2005. The reason for the change in trend observed after the anomaly is, at the moment, not understood. The elevation MIP had a significant variation until 12th December 2003 when a new PSO algorithm was activated in order to reduce the deviations of the ENVISAT platform attitude with respect to the nominal one. Similarly to the azimuth, after the anomaly of January 2005 the Elevation MIP has a drift that has no explanation. Investigations are ongoing to try to understand this behavior of the MIP as although it does not impact the data quality, it may invalidate attitude monitoring by GOMOS and could represent a hidden anomaly (section 4.6.3).

6

Radiometric sensitivity monitoring: for stars 25 and 9, the UV ratio is greater than the threshold 10%. It is clear that there is a global decrease of UV ratios for all the stars. This confirms the expected degradation suffered by the UV optics that is, anyway, very small considering also the small variation for the rest of the stars. For the photometers radiometric sensitivity ratios it is observed that every star has a variation that seems to be seasonally related. The variation is significant for stars 25 and 18. After some investigations performed by the QWG that exclude an inaccurate reflectivity correction LUT, it seems that the PH1/2 radiometric sensitivity variations could come from the fact that the spectrometers and the photometers are not illuminated the same way when the straylight appears (section 5.4.1).

Dark Charge calibration: new calibration ADF's (GOM_CAL_AX files) were disseminated during the reporting period with updated DC calibration maps (see dates and orbits used for the calibrations in section 5.1.2).

3   INSTRUMENT UNAVAILABILITY

3.1   GOMOS Unavailability Periods

There were no instrument unavailability periods during the reporting month.

3.2   Stars Lost in Centering

The acquisition of a star initiates with a rallying phase where the telescope mechanism is directed towards the expected position of the star. Subsequently the acquisition procedure enters into detection mode, where the SATU star tracker output signal is pre-processed for spot presence survey and for the location of the most illuminated couple of adjacent pixels for two added lines, over the detection field. The Most Illuminated Pixel (MIP) defines the position of the first SATU centering window. The following step in the acquisition sequence is then initiated and consists of a centering phase where the SATU output signal is pre-processed for spot presence survey over the maximum of 10x10 pixel field. This allows the third phase to begin: the tracking phase.

The centering phase has occasionally resulted in loss of the star from the field of view. Fig. 3.2-1 reports the percentage of the stars lost in centering for the period 03-FEB-2003 to 25-JUN-2006. It can be seen that only three stars, mainly weak stars (higher star id means higher magnitude) are lost during the centering phase between 4 and 6 % of their planned observations. The star id 115 was lost 9.5% of the times but it was planned to be occulted twenty one times and was lost twice (in period 19-25 January 2004), so this percentage of loss is not statistically significant.

As the monitoring shows neither a trend nor excessively high percentages of loss, there is no need for the moment to reject any star from the catalogue, and there is no indication of instrument-related problems.

Now with the instrument in a new operation scenario, the stars are also lost due to the anomaly "elevation voice coil command saturation" even if the instrument is not going anymore to Stand by / Refuse mode (section 3.3).

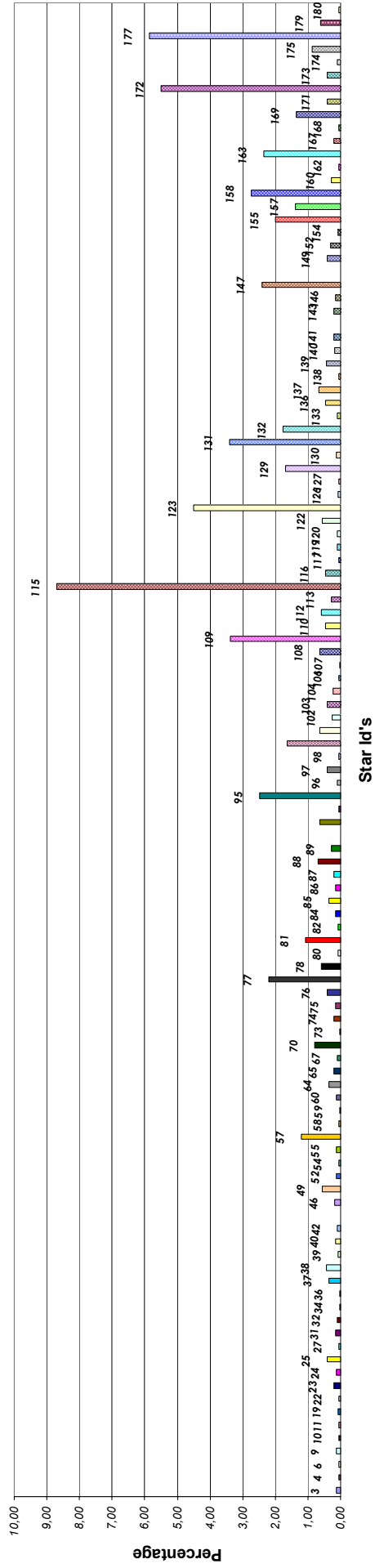## Statistics on stars lost in centering: 03-FEB-2003 until 25-JUN-2006

Figure 3.2-1: Statistics on stars that have been lost during the centering phase. The number above the columns correspond to the Star ID

3.3 Stars lost due to VCCS anomaly

No VCCS anomalies occurred during the reporting period.

3.4 Data Generation Gaps

The trend in percentage of available data within the archives PDHS-K and PDHS-E is depicted in fig. 3.4-1 (when instrument was in operation). It is a good indicator on how the PDS chain is working in terms of generation and dissemination of data to the archives. The percentage is calculated once per week.

For June the level 0 data availability is a little bit lower that nominal (~97%) due to an unavailability of ARTEMIS satellite with subsequent missing of dumped GOMOS data to ESRIN station. For level 1b the archived products are around 86%. The reason for the low statistics on level 1b products is that the allocated processing time is lower than the real processing time with the result that the end of the orbit is systematically not processed. Now the problem is known and is pending of resolution.

% of availability GOMOS occultations on the archives
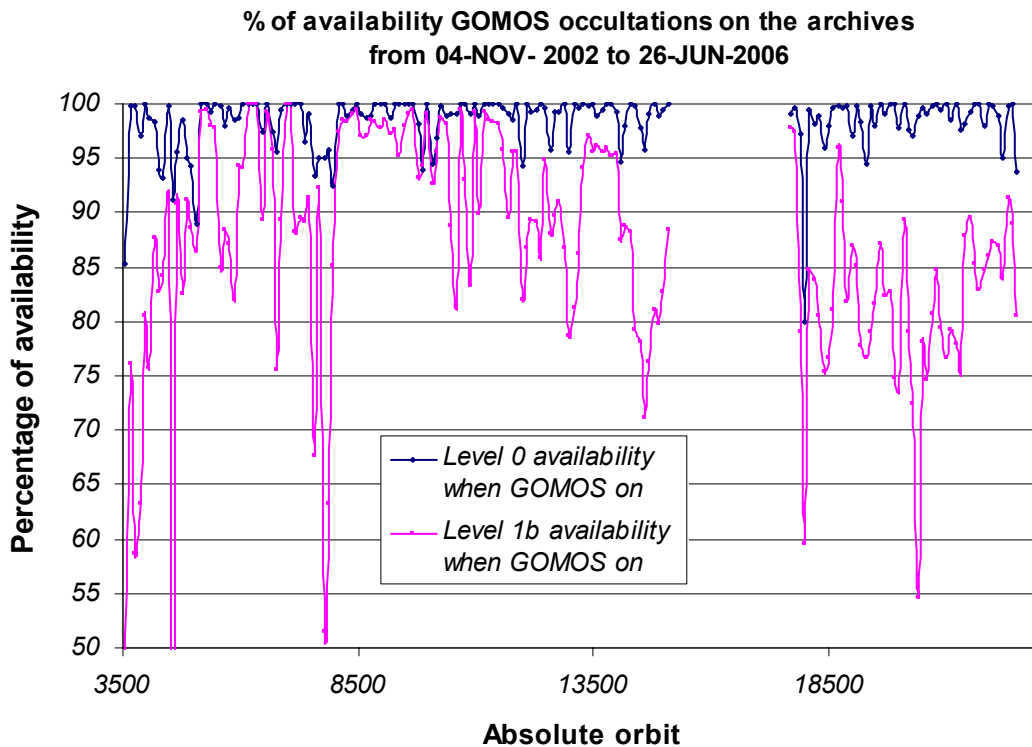**from 04-NOV- 2002 to 26-JUN-2006**

Figure 3.4-1: Percentage of level 0 and level 1b data availability on the archives PDHS-E and PDHS-K

3.4.1 LEVEL 0 PRODUCTS: GOM_NL__0P

Occultations planned to be acquired but for which no GOM_NL__0P data product has become available are presented in fig. 3.4-2 for the reporting period.
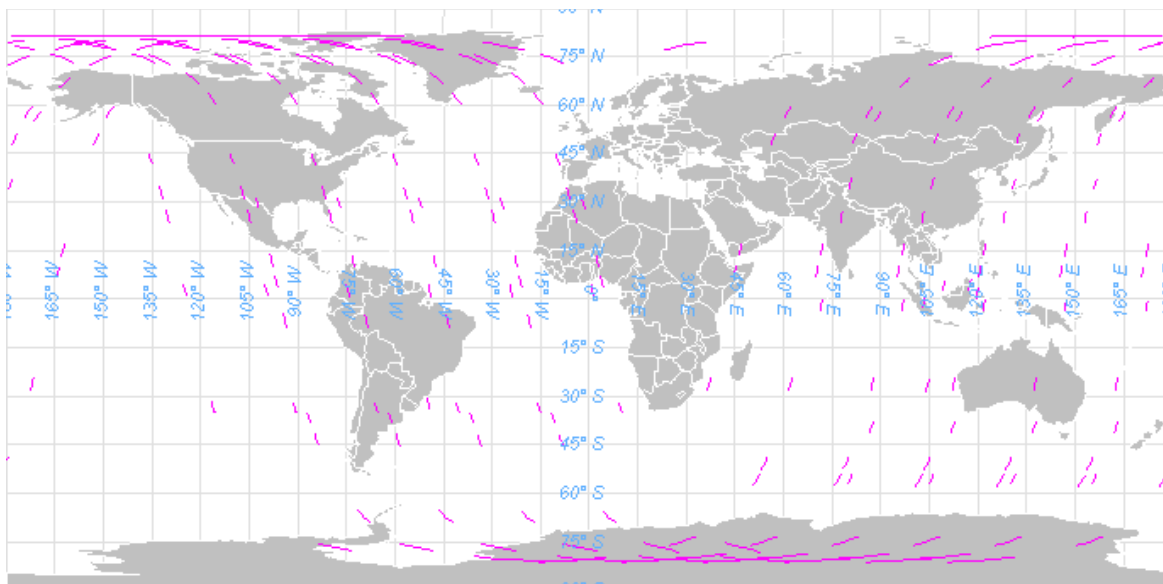
Figure 3.4-2: The pink lines are the orbit segments corresponding to planned data acquisitions for which no GOMOS level 0 product has become available

3.4.2 HIGHER LEVEL PRODUCTS

Routine dissemination of higher-level products produced by the PDS to the users is enabled. Reprocessed products (level 2) are available at D-PAC ftp server ftp-ops.de.envisat.esa.int from August 2002 to March 2006. Existing gaps will be covered by new products generated in 2006. The next operational processor (the current version is GOMOS 4.02, the next one will be GOMOS/5.00) that generates data in near real time will be in line with the prototype used for the reprocessing.

4   INSTRUMENT CONFIGURATION AND PERFORMANCE

4.1   *Instrument Operation and Configuration*

4.1.1 OPERATIONS SINCE BEGINNING OF MISSION

During the period end of March 2003 to July 2003 the azimuth range had to be decreased in steps (table 4.1-1) to avoid an instrument problem ("Voice_coil_command_saturation" anomaly) that caused GOMOS to go into STAND BY/REFUSE mode. On July 2003 the driver assembly was switched to the redundant B-side and since that date the full azimuth range (-10.8, +90.8) was again available until the second major anomaly occurred on 25th January 2005. Between this date and until the instrument was declared operational again (29th August 2005), GOMOS has been operated for testing and anomaly investigation purposes in different operations scenarios. The changes in azimuth configuration during the whole mission until end of reporting period are summarized in table 4.1-1.

Table 4.1-1: Historical changes in Azimuth configuration when GOMOS is in operations

Date	Orbit	Minimum Azimuth (°)	Maximum Azimuth (°)	Comment
01-MAR-2002		-10.8	+90.8	Nominal
29-MAR-2003 17:40	5635	0.0	+90.8	Reduced
31-MAY-2003 06:22	6530	+4.0	+90.8	Reduced
16-JUN-2003 16:17	6765	+12.0	+90.8	Reduced
15-JUL-2003 01:39	7200	-10.8	+90.8	Nominal
25-JAN-2005 23:33	15200	tests	tests	Different configuration for testing purposes
29-AUG-2005 02:52	18280	-10	+10	Reduced
26-SEP-2005 01:32	18680	-5	+20	Reduced
03-OCT-2005 01:12	18780	-5	+15	Reduced
09-OCT-2005 21:30	18878	-5	+20	Reduced
12-MAR-2006 17:29	21080	+10	+35	Reduced
09-APR-2006 12:47	21480	+5	+30	Reduced
16-APR-2006 15:48	21580	0	+25	Reduced
30-APR-2006 15:08	21780	-5	+20	Reduced
07-MAY-2006 14:48	21880	0	+25	Reduced
14-MAY-2006 14:28	21980	+15	+40	Reduced
28-MAY-2006 13:47	22180	+20	+45	Reduced
04-JUN-2006 13:27	22280	+15	+40	Reduced
18-JUN-2006 12:47	22480	+20	+45	Reduced
25-JUN-2006 12:27	22580	0	+25	Reduced
02-JUL-2006 12:07	22680	+5	+20	Reduced

4.1.2 CURRENT OPERATIONS AND CONFIGURATION

During the reporting period there were six synchronous sequences with occultations starting very high above the atmosphere in order to check the behaviour of the SATU oscillations at those altitude ranges. The ranges used were [280, 5], [200, 5] and [150, 5] km (see table 4.1-2).

The planned GOMOS operations for the reporting period are identified in table 4.1-2. The operation scenario of GOMOS since 29th August 2005 until end of reporting month consists of:

- Planning 2 orbits per sequence (nominal were 5): this is done because in case of a voice coil failure with subsequent loss of star observation, the maximum loss of consecutive observations cannot exceed two orbits.
- Reduced azimuth field of view (nominal was [-10°, +90°]): as the anomaly occurs during the rallying of the telescope in the preparation for the star observation, it has been decided to reduce the field of view in order to minimize the failure occurrence probability. Different ranges have been used during the reporting period (table 4.1-1) in order to optimize the number of occultations per orbit.

11

Table 4.1-2: GOMOS planned operations. The planning is built on a 2-orbit sequence basis (2 orbits with the same stars)

UTC Start	Start Orbit	Stop Orbit	Mode (Asynchronous or Synchronous)	Calibration (CAL) Dark Sky Area (DSA) or Nominal (Nom)
01-JUN-2006 01:37:56	22230	22321	S	Nom
07-JUN-2006 11:53:01	22322	22323	S	Nom; altitude range [280, 5] km
07-JUN-2006 15:14:13	22324	22335	S	Nom
08-JUN-2006 11:21:24	22336	22337	S	Nom; altitude range [200, 5] km
08-JUN-2006 14:42:36	22338	22349	S	Nom
09-JUN-2006 10:49:47	22350	22351	S	Nom; altitude range [150, 5] km
09-JUN-2006 14:10:59	22352	22363	S	Nom
10-JUN-2006 10:18:10	22364	22365	S	Nom; altitude range [280, 5] km
10-JUN-2006 13:39:22	22366	22375	S	Nom
11-JUN-2006 06:25:21	22376	22377	S	Nom; altitude range [200, 5] km
11-JUN-2006 13:07:45	22380	22387	A	CAL78
12-JUN-2006 02:32:32	22388	22393	S	Nom
12-JUN-2006 12:36:08	22394	22395	S	Nom; altitude range [150, 5] km
12-JUN-2006 15:57:20	22396	22659	S	Nom

There was no new Configurable Table Interface (CTI) uploaded to the instrument. The files used since the beginning of the mission are in table 4.1-3.

Table 4.1-3: Historic CTI Tables

CTI filename	Dissemination to FOCC
CTI_SMP_GMVIEC20030716_123904_00000000_00000004_20030715_000000_20781231_235959.N1	16-JUL-2003
CTI_SMP_GMVIEC20021104_075734_00000000_00000003_20021002_000000_20781231_235959.N1	06-NOV-2003
CTI_SMP_GMVIEC20021002_082339_00000000_00000002_20021002_000000_20781231_235959.N1	07-OCT-2003
CTI_SMP_GMVIEC20020207_154455_00000000_00000000_20020301_032709_20781231_235959.N1	21-FEB-2002

4.2   Limb, Illumination conditions and instrument gain setting

The **limb** and the **illumination condition** are two parameters that can confuse the user community. In table 4.2-1 there are specified the product parameter (level 1b and level 2 of operational processor GOMOS/4.02) where the flag is located, the meaning and the source. The difference between the limb (SPH/bright_limb) and the illumination condition (SUMMARY_QUALITY/limb_flag) is that the first one is coming from the mission scenario and the second is coming from the processing (defined from the computation of the sun

zenith and azimuth angles at both instrument and tangent point locations). The SPH/bright_limb is for some occultations set to "dark" in the mission scenario while they are in fact in bright limb illumination conditions. To select the highest quality data for scientific applications, data with SUMMARY_QUALITY/limb_flag equal to '0' should be used (see also the disclaimer: http://envisat.esa.int/dataproducts/availability/disclaimers). The instrument gain settings are also specified in table 4.2-1 (they depend on the mission scenario flags) just for completeness of information.

Table 4.2-1: Relationship between limb, illumination condition flags and instrument gain settings (operational IPF version GOMOS/4.02)

Products parameter	SPH/bright_limb	0 = Dark	1 = Bright	Coming from mission scenario
	SUMMARY_QUALITY/limb_flag	0 = Full Dark 1 = Bright 2 = Twilight	1 = Bright 2 = Twilight	In the geolocation process the sun zenith angle is computed and the occultation then is flagged accordingly
Instrument Gain	SPA Gain	3 (2)	0	Gain setting for spectrometer A. In parenthesis, values valid only for Sirius occultations (starID=1)
	SPB Gain	0	0	Gain setting for spectrometer B

The same is valid for the prototype version GOPR_6.0a_6.0a and following ones (including the one that is used for the on-going second reprocessing of 2002-2005 years), where the **limb** is in fields SPH/bright_limb and SUMMARY_QUALITY/dark_bright_limb and the **illumination condition** is in field SUMMARY_QUALITY/obs_ill_cond. For these prototypes, the illumination condition can have five values (see table 4.2-2).

Table 4.2-2: Relationship between limb, illumination condition flags and instrument gain settings (prototype version GOPR 6.0a_6.0a and following ones)

Products parameter	SPH/bright_limb SUMMARY_QUALITY/dark_bright_limb	0 = Dark	1 = Bright	Coming from mission scenario
	SUMMARY_QUALITY/obs_ill_cond	0 = Full Dark 1 = Bright 2 = Twilight 3 = Straylight 4 = Twi.+Stray.		In the geolocation process the sun zenith angle is computed and the occultation is then flagged accordingly
Instrument Gain	SPA Gain	3 (2)	0	Gain setting for spectrometer A. In parenthesis, values valid only for Sirius occultations (starID=1)
	SPB Gain	0	0	Gain setting for spectrometer B

4.3   *Thermal Performance*

Since the beginning of the mission, the hot pixel and RTS phenomena have been producing a continuous increase of the dark charge signal within the CCD detectors (see section 4.5.1). In order to minimize this

effect, three successive CCD cool downs were performed in orbits 800 (25th April 2002), 1050 (13th May 2002) and 2780 (11th September 2002) with a total decrease in temperature of 14 degrees.

Fig. 4.3-1 and 4.3-2 display, respectively, the overall temperature variation and the temperature variation around the Ascending Node Crossing (ANX) time with a resolution of 0.4 degrees (coding accuracy for level 0 data). The CCD temperatures show the expected global increase due to the radiator ageing.
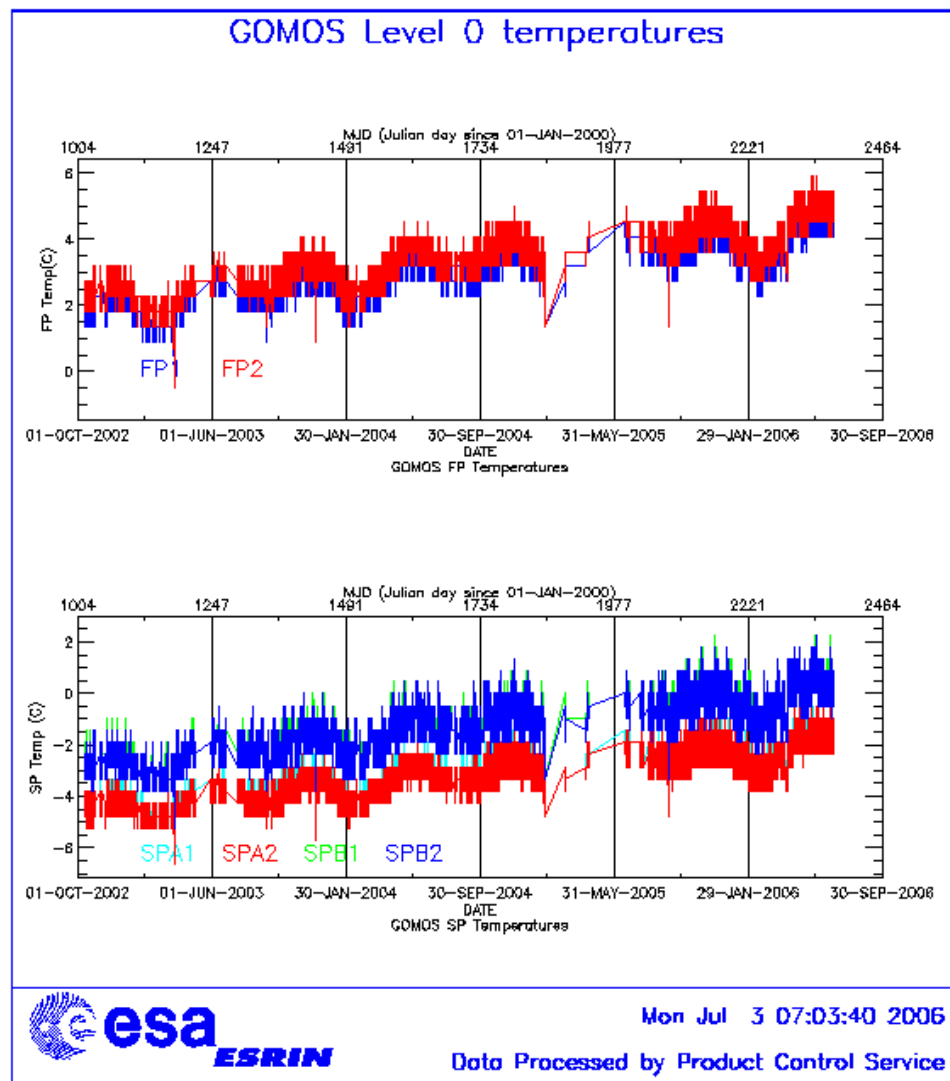

Figure 4.3-1: Level 0 temperature evolution of all GOMOS CCD detectors since October 2002 until the end of the reporting period

Another expected variation of the temperatures, the seasonal one, with amplitude of around 0.8 degrees, can be also observed. The peaks that occur mainly in spectrometer B1 and B2 are also to be noted. They happen a little before the ANX for some consecutive orbits and every 8-10 days. Their origin is not known, as we did not find any correlation between these peaks and other activities carried out by other ENVISAT instruments. The CCD temperature at almost the same latitude location (fig. 4.3-2) is monitored in order to

14

detect any inter-orbital temperature variation. The abnormal decreases observed sometimes in all detectors are after GOMOS switch off periods, when the instrument did not have enough time to reach the nominal temperature before starting the measurements.
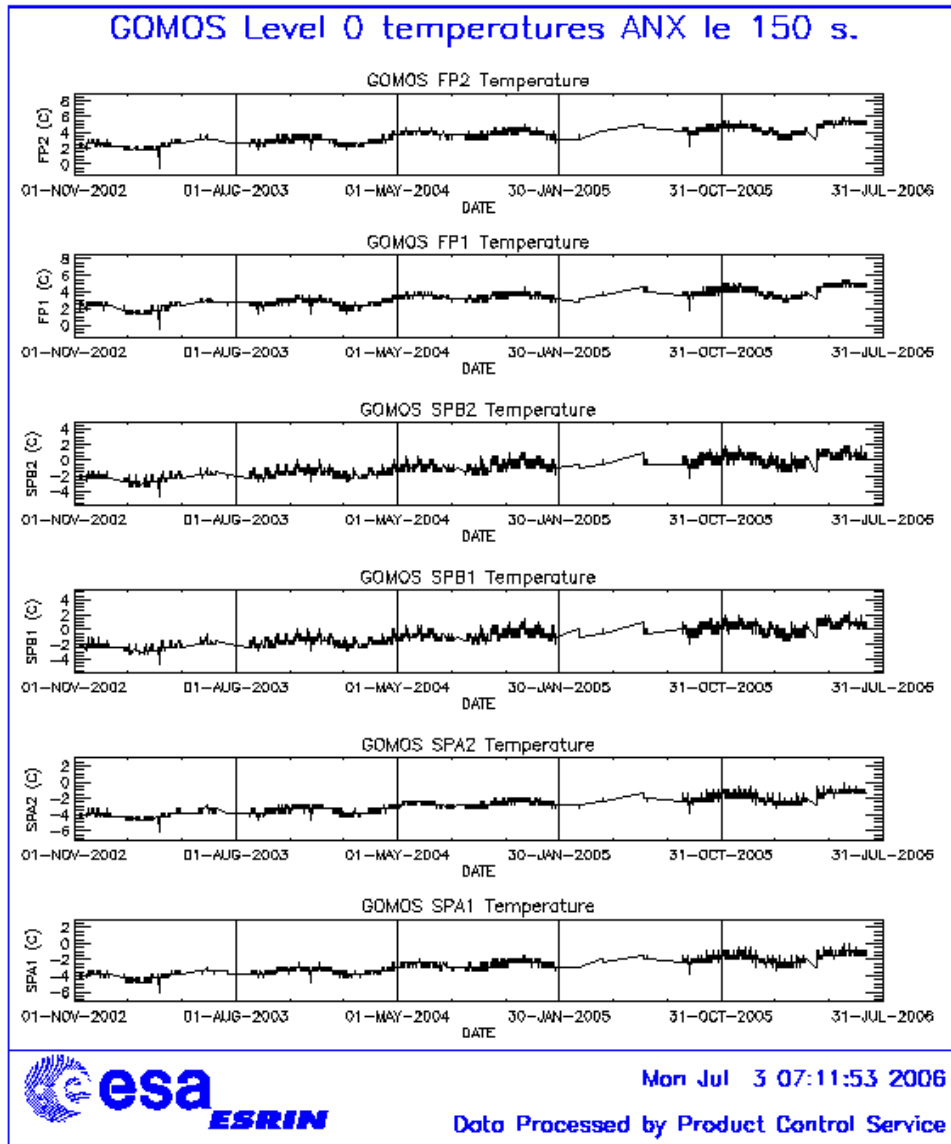

Figure 4.3-2: Level 0 temperature evolution of all GOMOS CCD detectors around ANX since November 2002 until the end of the reporting period

During June 2006, the orbital temperature variation of the detector SPB2 for ascending and descending passes (fig. 4.3-3 and 4.3-4) is nominal, around 2.5-3 degrees. The stability of the temperature during the orbit is important because it affects the position of the interference patterns. The phenomenon of the interference is present mainly in SPB and this Pixel Response Non-Uniformity (PRNU) is corrected during the processing.
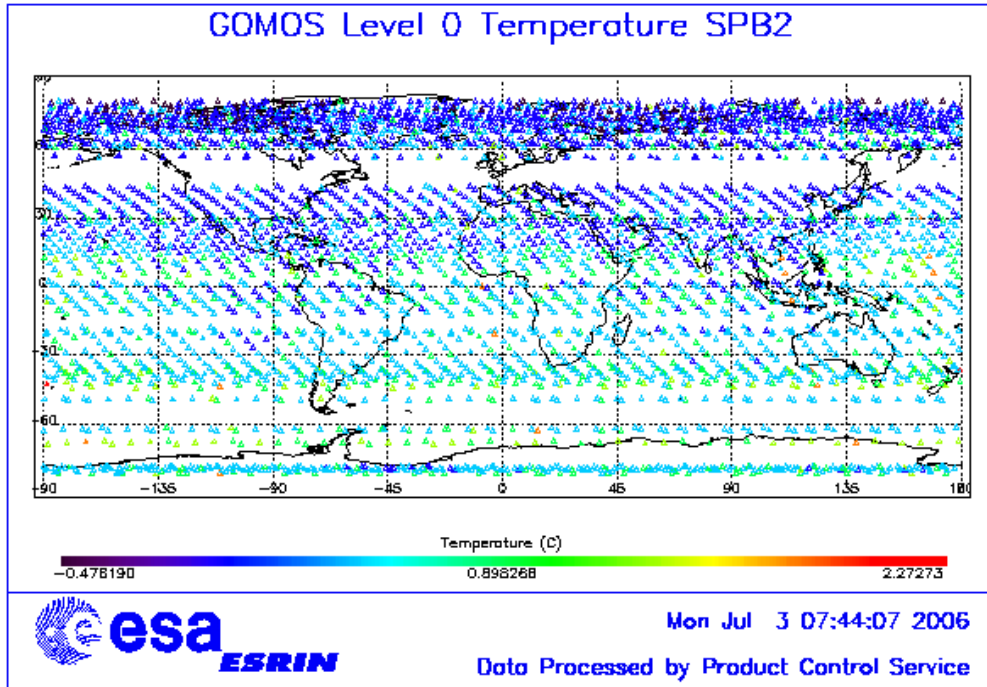
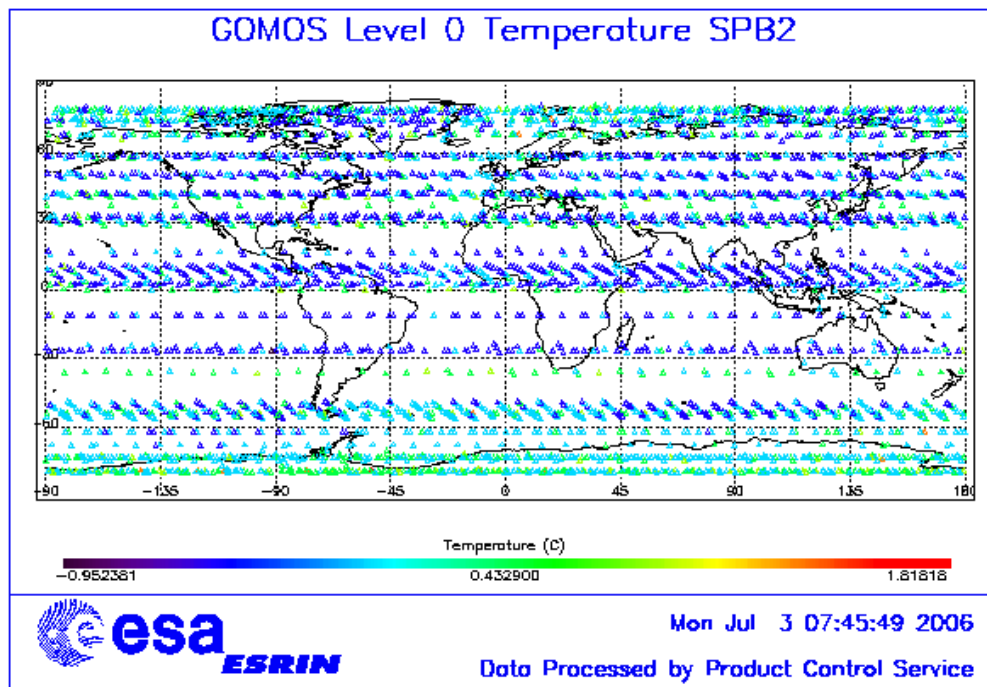**Figure 4.3-3: Ascending orbital variation of SPB2 temperature during reporting period**

Figure 4.3-4: Descending orbital variation of SPB2 temperature during reporting period

4.4 Optomechanical Performance

New band setting calibration has been performed during the reporting period.

- Version GOMOS/4.00 and previous ones: in the GOMOS processor versions GOMOS/4.00 and previous, the spectra are expected to be aligned along CCD lines, and therefore use only a single average line index per CCD. In table 4.4-1, the mean values of the location of the star signal for all the calibration analysis done is reported. The 'left' and 'right' values are calculated (the whole interval is not used) because the spectra present a slight slope, more pronounced in spectrometer B (see fig. 4.4-1). In table 4.4-2, mean values of the location of the star signal are calculated for some specific wavelength intervals. These intervals have been changed between the calibration performed in September 2002 and the ones performed afterwards (until November 2003). Table 4.4-3 reports the average location of the star spot on the photometer 1 and 2 CCD.

- Version GOMOS/4.02: in the current processor version (GOMOS/4.02) operational since 23rd March 2004, a Look Up Table (LUT) gives the line index of the spectra location as a function of the wavelength (blue dots in fig. 4.4-1). However this characterization curve is not exactly the location of the star spectrum on the CCD but rather a combination of this position and some artefact created by the shape of the instrument optical point spread function. The exact shape is actually a straight line (especially for SPB) that has been characterised in 2005 and will be implemented in next updates of GOMOS ADF's. In the meantime calibration exercises should be performed in order to check if the LUT values are still valid.
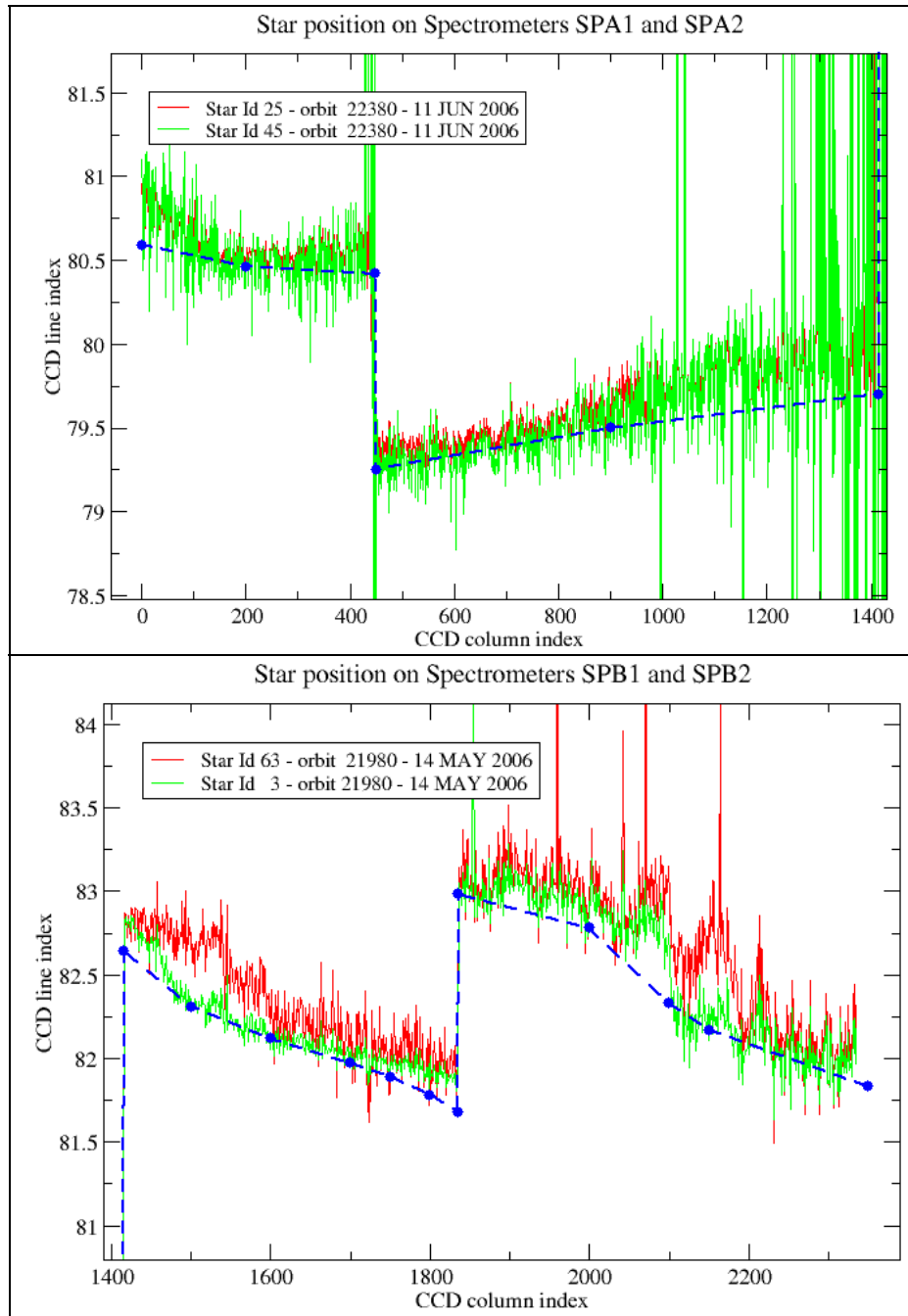
Figure 4.4-1: Average position of star spectra on the CCD for SPA (upper) and SPB (lower)

A calibration exercise was performed using data of May and June 2006. The position of the stellar spectra of star id 25 and 45 for SPA1/SPA2 and star id 63 and 3 for SPB1/SPB2 (fig. 4.4-1) observed in dark-limb spatial spread monitoring mode have been averaged above 120 km altitude and compared to the values of the LUT. The results confirm the LUT values (see table 4.4-4) which means that for the time being there is no need to update the table.

Table 4.4-1: Mean value of the location of the star signal during the occultation at the edges of every band (mean over 50 values, filtering the outliers)

	UV (SPA1) left/right	VIS (SPA2) left/right (Inverted spectra)	IR1 (SPB1) left/right	IR2 (SPB2) left/right
11/09/2002	80.7/80.7	79.8/79.5	82.8/81.9	83.1/82.1
01/01/2003	80.7/80.6	79.8/79.5	82.8/82.0	83.2/82.2
17/07/2003 & 02/08/2003	80.7/80.7	79.8/79.5	82.8/81.9	83.1/82.1
08/11/2003	80.7/80.6	79.8/79.5	82.8/81.9	83.1/82.1

Table 4.4-2: Mean value of the location of the star signal during the occultation (as table 4.4-1) but now within some wavelength intervals

	UV (SPA1)	VIS (SPA2)	IR1 (SPB1)	IR2 (SPB2)
11/09/2002 wl range (nm)	80.8 [300-330]	79.8 [500-530]	82.6 [760-765]	82.9 [937-942]
01/01/2003 wl range (nm)	80.6 [350-360]	78.6 [650-670]	81.6 [760-765]	80.3 [935-945]
02/08/2003	80.6	79.7	82.5	82.8
08/11/2003	80.6	79.9	82.4	82.8

Table 4.4-3: Average column and row pixel location of the star spot on the photometer CCD during the occultation

	FP1 (column/row)	FP2 (column/row)
11/09/2002	11/4	5/5
01/01/2003	10/4	6/4.9
02/08/2003	10/4	6/5
08/11/2003	10/4	6/5

Table 4.4-4: Location of the star signal on the CCD's (corresponding to fig. 4.4-1)

Pixel Column	LUT (Pixel line)	Calibration on 10-APR-2004	Calibration on 04-DEC-2004	Calibration on 27-NOV-2005	Calibration on 19-FEB-2006	Calibration on 14-MAY-2006 and 11-JUN-2006
0	80.59	80.80	80.67	80.93	80.67	80.85
20	80.46	80.60	80.44	80.32	80.43	80.49
449	80.42	80.50	80.42	80.40	80.53	80.56
450	79.25	79.39	79.30	79.16	79.30	79.35
900	79.50	79.63	79.57	79.36	79.45	79.61
1415	79.70	79.76	79.76	80.00	79.81	79.93
1416	82.64	82.80	82.88	82.95	82.76	82.81
1500	82.31	82.60	82.66	82.63	82.58	82.55
1600	82.12	82.22	82.30	82.35	82.41	82.20
1700	81.97	82.04	82.08	82.09	82.05	82.06
1750	81.89	81.98	82.03	82.00	81.92	81.97
1800	81.78	81.91	81.96	81.93	81.83	81.98
1835	81.68	81.88	81.94	81.96	81.79	81.91
1836	82.98	83.10	83.10	83.27	83.17	83.08
2000	82.78	82.90	82.94	83.04	82.83	82.93
2100	82.33	82.70	82.73	82.82	82.83	82.67
2150	82.17	82.40	82.54	82.79	82.70	82.49
2350	81.83	82.00	82.00	82.68	81.96	82.11

4.5   Electronic Performance

4.5.1 DARK CHARGE EVOLUTION AND TREND

The trend of Dark Charge (DC) is of crucial importance for the final quality of the products, and is therefore subject to intense monitoring. As part of the DC there is:

- "Hot pixels", a pixel is "hot" when its dark charge exceeds its value measured on ground, at the same temperature, by a significant amount.
- RTS phenomenon (Random Telegraphic Signal), it is an abrupt change (positive or negative) of the CCD pixel signal, random in time, affecting only the DC part of the signal and not the photon generated signal.

The temperature dependence of the DC would make this parameter a good indicator of the DC behaviour, but the hot pixels and the RTS are producing a continuous increase of the DC (see trend in fig. 4.5-1 and 4.5-2). To take into account these phenomena, since version GOMOS/4.00 (the current one is GOMOS/4.02) a DC map per orbit is extracted from a Dark Sky Area (DSA) observation performed around ANX (full dark conditions). For every level 1b product (occultation), the actual thermistor temperature of the CCD is used to convert the DC map measured around ANX into an estimate of the DC at the time (and different temperature) of the actual occultation. When the DSA observation is not available, the DC map inside the calibration product that was measured at a given thermistor reference temperature is used; again, the actual thermistor temperature of the CCD is used to compute the actual map. Table 4.5-1 reports the list of products that used the DC maps inside the calibration file due to the non-availability of DSA observation. A "CAL DC map with no T dep." means that, as the temperature information was not available for that occultation, the DC map used is exactly the one inside the Calibration product.

The "quality ranking" of the products depending on DC correction performed is as follows:
- Best quality: products with DC correction using DSA observation inside the orbit
- Less quality than previous ones: products with DC correction using the map inside the calibration product, thermal corrected ('DC map used' in table 4.5-1)
- Less quality than previous ones: products with DC correction using the map inside the calibration product, no thermal corrected ('DC map with no T dep.' in table 4.5-1)

Table 4.5-1: Table of level 1b products that used the Calibration DC maps instead of the DSA observation

Product name	DC information
GOM_TRA_1PNPDE20060603_030520_000000352048_00161_22259_0000.N1	DC map used
GOM_TRA_1PNPDE20060603_205931_000000462048_00172_22270_0000.N1	DC map used
GOM_TRA_1PNPDE20060603_210118_000000472048_00172_22270_0001.N1	DC map used
GOM_TRA_1PNPDE20060603_210500_000000432048_00172_22270_0002.N1	DC map used
GOM_TRA_1PNPDE20060603_210833_000000452048_00172_22270_0003.N1	DC map used
GOM_TRA_1PNPDE20060603_211023_000000412048_00172_22270_0004.N1	DC map used
GOM_TRA_1PNPDE20060603_211233_000000392048_00172_22270_0005.N1	DC map used
GOM_TRA_1PNPDE20060603_212029_000000412048_00172_22270_0006.N1	DC map used
GOM_TRA_1PNPDE20060612_193700_000000442048_00300_22398_0000.N1	DC map used
GOM_TRA_1PNPDE20060612_193844_000000452048_00300_22398_0001.N1	DC map used

GOM_TRA_1PNPDE20060612_194007_000000482048_00300_22398_0002.N1	DC map used
GOM_TRA_1PNPDE20060612_194528_000000392048_00300_22398_0003.N1	DC map used
GOM_TRA_1PNPDE20060612_194713_000000362048_00300_22398_0004.N1	DC map used
GOM_TRA_1PNPDE20060612_195642_000000392048_00300_22398_0005.N1	DC map used
GOM_TRA_1PNPDE20060612_195948_000000372048_00300_22398_0006.N1	DC map used
GOM_TRA_1PNPDE20060612_200647_000000412048_00300_22398_0007.N1	DC map used
GOM_TRA_1PNPDE20060612_202346_000000582048_00300_22398_0008.N1	DC map used
GOM_TRA_1PNPDE20060612_202948_000000402048_00300_22398_0009.N1	DC map used
GOM_TRA_1PNPDE20060616_205346_000000442048_00358_22456_0000.N1	DC map used
GOM_TRA_1PNPDE20060616_205509_000000462048_00358_22456_0001.N1	DC map used
GOM_TRA_1PNPDE20060616_210019_000000392048_00358_22456_0002.N1	DC map used
GOM_TRA_1PNPDE20060616_210649_000000422048_00358_22456_0003.N1	DC map used
GOM_TRA_1PNPDE20060616_210919_000000432048_00358_22456_0004.N1	DC map used
GOM_TRA_1PNPDE20060616_211120_000000372048_00358_22456_0005.N1	DC map used
GOM_TRA_1PNPDE20060616_211421_000000382048_00358_22456_0006.N1	DC map used
GOM_TRA_1PNPDE20060616_212108_000000412048_00358_22456_0007.N1	DC map used
GOM_TRA_1PNPDE20060617_202213_000000442048_00372_22470_0000.N1	DC map used
GOM_TRA_1PNPDE20060617_202337_000000472048_00372_22470_0001.N1	DC map used
GOM_TRA_1PNPDE20060617_202844_000000372048_00372_22470_0002.N1	DC map used
GOM_TRA_1PNPDE20060617_203509_000000422048_00372_22470_0003.N1	DC map used
GOM_TRA_1PNPDE20060617_203739_000000422048_00372_22470_0004.N1	DC map used
GOM_TRA_1PNPDE20060620_202803_000000482048_00415_22513_0000.N1	DC map used
GOM_TRA_1PNPDE20060620_202930_000000482048_00415_22513_0001.N1	DC map used
GOM_TRA_1PNPDE20060620_203047_000000462048_00415_22513_0002.N1	DC map used
GOM_TRA_1PNPDE20060620_204047_000000402048_00415_22513_0003.N1	DC map used
GOM_TRA_1PNPDE20060620_204314_000000402048_00415_22513_0004.N1	DC map used
GOM_TRA_1PNPDE20060620_205457_000000402048_00415_22513_0005.N1	DC map used
GOM_TRA_1PNPDE20060620_210458_000000462048_00415_22513_0006.N1	DC map used
GOM_TRA_1PNPDE20060623_024346_000000432048_00447_22545_0000.N1	DC map used
GOM_TRA_1PNPDE20060624_200230_000000452048_00472_22570_0000.N1	DC map used
GOM_TRA_1PNPDE20060624_200354_000000482048_00472_22570_0001.N1	DC map used
GOM_TRA_1PNPDE20060624_200603_000000482048_00472_22570_0002.N1	DC map used
GOM_TRA_1PNPDE20060624_201449_000000392048_00472_22570_0003.N1	DC map used
GOM_TRA_1PNPDE20060624_201712_000000372048_00472_22570_0004.N1	DC map used
GOM_TRA_1PNPDE20060624_202645_000000442048_00472_22570_0005.N1	DC map used
GOM_TRA_1PNPDE20060624_202849_000000392048_00472_22570_0006.N1	DC map used
GOM_TRA_1PNPDE20060624_203827_000000452048_00472_22570_0007.N1	DC map used
GOM_TRA_1PNPDE20060624_204531_000000442048_00472_22570_0008.N1	DC map used
GOM_TRA_1PNPDE20060624_204705_000000472048_00472_22570_0009.N1	DC map used
GOM_TRA_1PNPDE20060624_205252_000000512048_00472_22570_0010.N1	DC map used
GOM_TRA_1PNPDE20060624_205519_000000462048_00472_22570_0011.N1	DC map used
GOM_TRA_1PNPDE20060626_203058_000000412048_00501_22599_0000.N1	DC map with no T dep.
GOM_TRA_1PNPDE20060628_211402_000000382049_00029_22628_0000.N1	DC map used
GOM_TRA_1PNPDE20060628_211550_000000422049_00029_22628_0001.N1	DC map used
GOM_TRA_1PNPDE20060628_211730_000000432049_00029_22628_0002.N1	DC map used
GOM_TRA_1PNPDE20060628_211854_000000462049_00029_22628_0003.N1	DC map used
GOM_TRA_1PNPDE20060628_212344_000000362049_00029_22628_0004.N1	DC map used
GOM_TRA_1PNPDE20060628_212529_000000352049_00029_22628_0005.N1	DC map used
GOM_TRA_1PNPDE20060628_212929_000000372049_00029_22628_0006.N1	DC map used
GOM_TRA_1PNPDE20060628_213150_000000372049_00029_22628_0007.N1	DC map used
GOM_TRA_1PNPDE20060628_213426_000000342049_00029_22628_0008.N1	DC map used
GOM_TRA_1PNPDE20060628_213712_000000362049_00029_22628_0009.N1	DC map used

GOM_TRA_1PNPDE20060628_214321_000000372049_00029_22628_0010.N1	DC map used
GOM_TRA_1PNPDE20060628_214538_000000362049_00029_22628_0011.N1	DC map used
GOM_TRA_1PNPDE20060628_214933_000000332049_00029_22628_0012.N1	DC map used
GOM_TRA_1PNPDE20060628_215351_000000342049_00029_22628_0013.N1	DC map used
GOM_TRA_1PNPDE20060628_220410_000000392049_00029_22628_0014.N1	DC map used
GOM_TRA_1PNPDE20060628_220550_000000332049_00029_22628_0015.N1	DC map used
GOM_TRA_1PNPDE20060628_220759_000000372049_00029_22628_0016.N1	DC map used
GOM_TRA_1PNPDE20060628_221911_000000402049_00029_22628_0017.N1	DC map used
GOM_TRA_1PNPDE20060628_222258_000000382049_00029_22628_0018.N1	DC map used
GOM_TRA_1PNPDE20060630_200535_000000412049_00057_22656_0000.N1	DC map with no T dep.
GOM_TRA_1PNPDE20060630_201055_000000382049_00057_22656_0001.N1	DC map used

The average DC inserted by the processor into the level 1b data products for the spectrometers SPA1 and SPB2 (per band: upper, central and lower) is plotted in fig. 4.5-1 and 4.5-2. From the figures, it can be noted that the DC is increasing at a slightly higher rate than for previous years: 500 electrons per year for SPA1 and 700 electrons per year for SPB2.

The same DC values are plotted in fig. 4.5-3 but for some occultations belonging only to the reporting month.
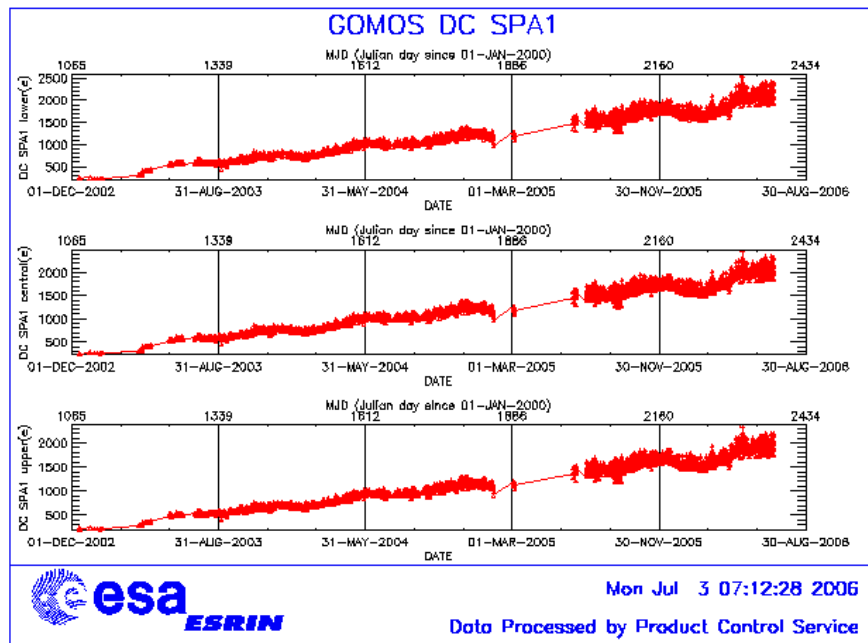

Figure 4.5-1: Mean DC evolution on SPA1 since 15th December 2002 until the end of the reporting period
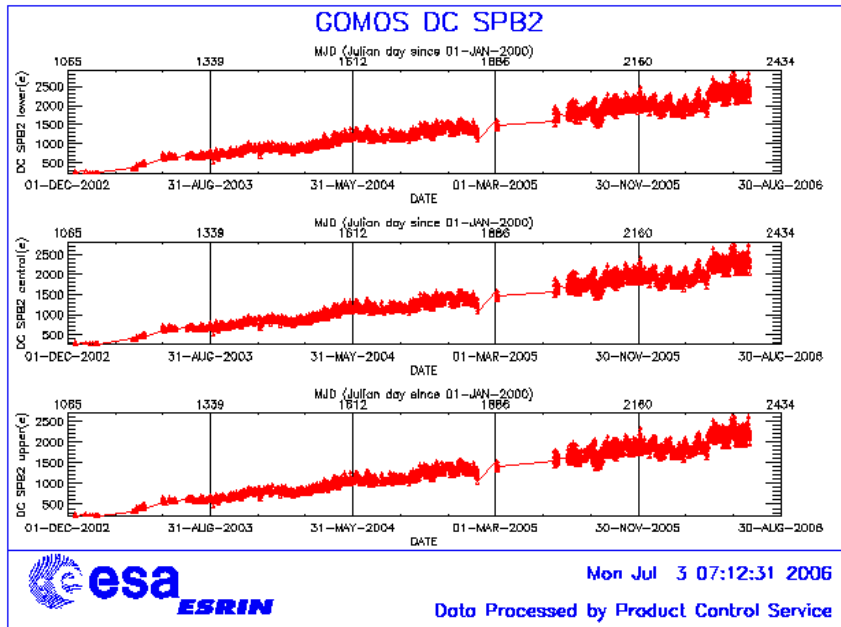
Figure 4.5-2: Mean DC evolution on SPB2 from 15th December 2002 until the end of the reporting period
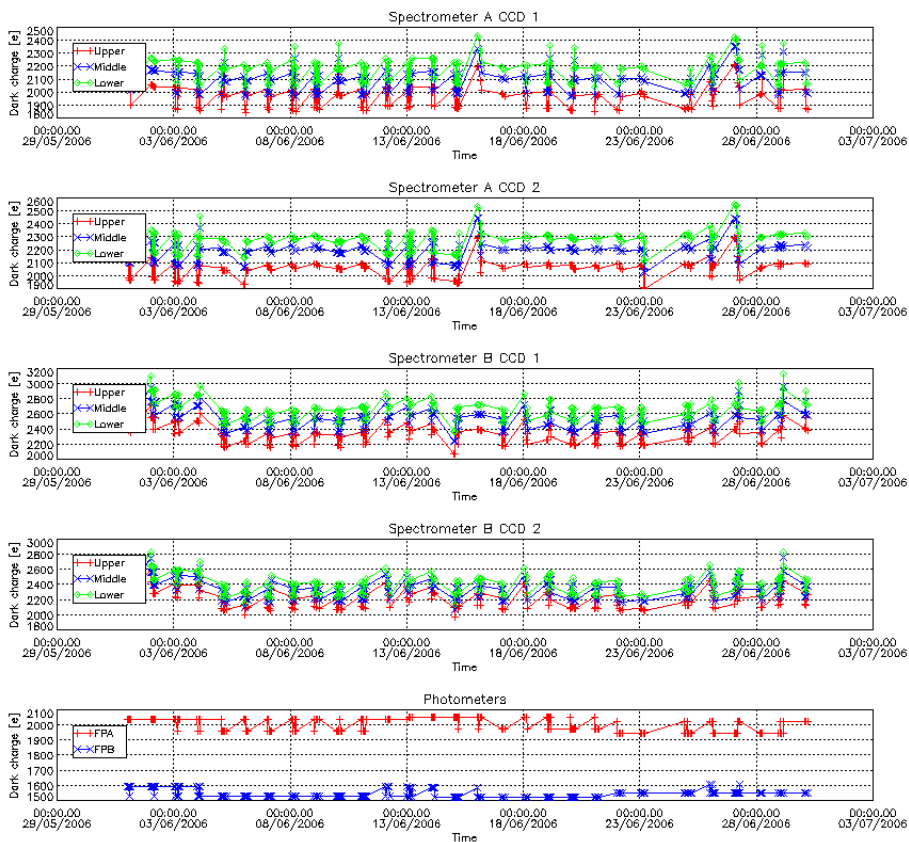

Figure 4.5-3: Mean Dark Charge of spectrometers and photometers during the reporting period

23

4.5.2 SIGNAL MODULATION

A parasitic signal was found to be systematically present, added to the useful signal, for the spectrometers A and B. The modulation is corrected in the data processing for spectrometers A1 and A2 (for spectrometer B it has much smaller amplitude and so is not corrected) and the modulation signal standard deviation is routinely monitored in order to detect any trend (fig. 4.5-4).

The modulation standard deviation, for every spectrometer, is characterised as follows:

$$\sigma_{mod} = (\text{'static noises'} - \text{'total static variance'})^{1/2} / \text{gain} \qquad (\text{in ADU})$$

- The 'static noises' are calculated from the DSA observation performed once per orbit
- The 'total static variance' is obtained from ADF data (electronic chain noise, quantization noise).

The standard deviation of the modulation signal (fig. 4.5-4) shows high values during summer time for the ESRIN data, it now being confirmed that the South Atlantic Anomaly is the cause of these unexpected peaks. The quality of ESRIN data, in particular over the SAA zone, is impacted but the measure of this impact is under investigation. However, in the second half of October (both 2004 and 2005) the peaks are smaller because the DSA zone where the data are taken for this analysis is moving towards the Northern Hemisphere. At the end of October the DSA zone is definitely chosen by the planning system in the Northern Hemisphere (to fill the criteria 'DSA in full dark limb conditions') and the high peaks disappear.
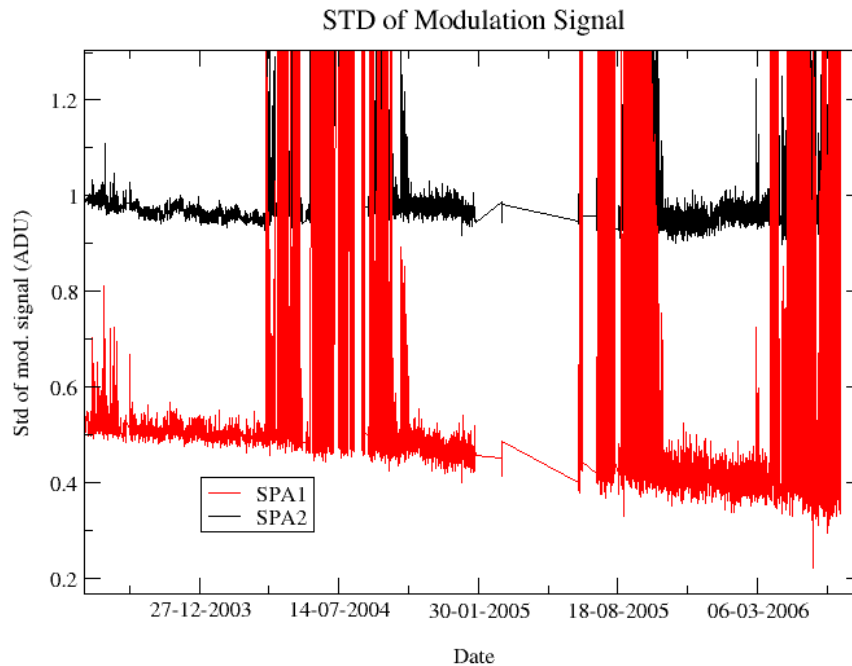

Figure 4.5-4: Standard deviation of the modulation signal

4.5.3 ELECTRONIC CHAIN GAIN AND OFFSET

No new electronic chain gain and offset calibration has been done during the reporting period so the results have been presented in previous MR.

The routine monitoring of the ADC offset is a good indicator of the ageing of the instrument electronics. During November 2005 an exercise has been done to analyze the variation of the ADC offset using the calibration observation in linearity mode performed on 28th November 2005.

The fig. 4.5-5 presents the evolution of the calibrated ADC offset for each spectrometer electronic chain. The unexpected increase of this offset seems to be due to an external contribution. In the ADC offset calibration procedure, linearity observations are used with two integration times of 0.25 and 0.50 seconds to extrapolate to an integration time of 0 seconds that gives the complete chain offset and not only the ADC offset. The complete offset contains any possible offsets, and especially the static dark charge (i.e. the dark charge that does not depend on the spectrometer integration time). If the memory area of the CCD is affected by the generation of hot pixels (this is confirmed by the presence of vertical lines visible in the measurement maps in spatial spread monitoring mode), it can be concluded that the increase observed in fig. 4.5-5 is due to these new hot pixels.
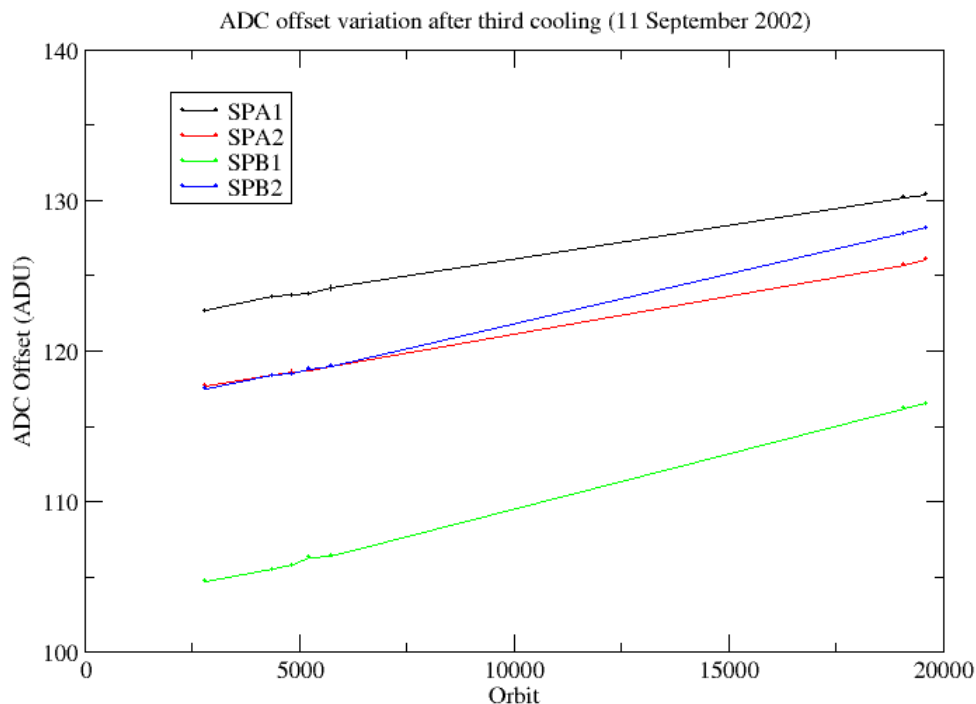

Figure 4.5-5: Evolution of the ADC offset for each spectrometer electronic chain

A current QWG task consists in completing the analysis to confirm that the offset increase is due to the dark charge increase in the memory area. This can be proven by the study of the noise due to the increased dark charge. The increase of ADC offset will be assumed to be equal to the increase of 'static dark charge' and

the corresponding noise will be computed and compared to the increase of the residual of the signal variance.

If we keep the ADC offset constant, as it is also used to compute the dark charge at band level (which is used to correct the samples in the level 1b processing), the increase of the static dark charge - not taken into account in the ADC offset - is compensated by an artificial increase of the calibrated dark charge. So, the star and limb spectra are correctly corrected for dark charge. A small bias can be added to the instrument noise due to the incorrect dark charge level. Anyway, this quantity is not large enough to require a modification of the ADC offset value.

An electronic chain gain calibration exercise has been performed. The values obtained have been compared with the ones written in the ADF and used by the operational IPF. The relative difference is much less than the 20% (threshold to change the ADF values) and thus no update of the gain is foreseen after this analysis.

4.6   Acquisition, Detection and Pointing Performance

4.6.1 SATU NOISE EQUIVALENT ANGLE

The Star Acquisition and Tracking Unit (SATU) noise equivalent angle (SATU NEA) consists of the statistical angular variation of the SATU data above the atmosphere. The mean of the standard deviation (STD over the 50 values per measurement) above 105 km are computed for every occultation, giving two values per occultation: one in the 'X' direction, one in the 'Y' direction. A mean value per day in every direction and limb is calculated and monitored in order to assess instrument performance in terms of star pointing (fig. 4.6-1, upper). Also monthly averages are calculated and plotted (fig. 4.6-2). The thresholds are 2 and 3 micro radians in 'X' and 'Y' directions respectively. Before May 2003, data above 90 km have been considered (instead of 105 km) but from May 2003 on, data taken in the mesospheric oxygen layer (located around 100 km altitude) have been avoided because they could cause fluctuations on the SATU data. Also the products with errors (error flag set) are discarded from May 2003 onwards.

As can be seen in fig. 4-6.1-upper, the SATU NEA had a sudden increase on 8th September 2005 mainly in 'Y' axis. These values remained high, fluctuating between 1 and 1.8 microrad until December 2005 when they came back to the values they used to be before the increase of September. The reason why there was higher noise in the data causing the jump in daily SATU average is not known. Now a different problem has been present since mid April 2006. A gradual increase of the daily SATU Y mean is observed. This increase is due to fluctuations of the SATU 'Y' data observed at the beginning of the occultations (starting at 130 km that corresponds to an elevation angle of around 65°). Special occultations have been performed starting at 280/250/200 km in order to check at which angle the fluctuations start but surprisingly there are two elevation angle ranges for which the fluctuations appear (see fig. 4.6-2-lower). Preliminary investigations carried out by the ESL, ESA and industry point to a problem on the SFM (mechanical or electrical) and not to a problem on the SATU itself. Since mid June the increase seems to be stable at around 5.5 micro radians. Future monthly reports will inform on the status of this anomaly which is carefully monitored.
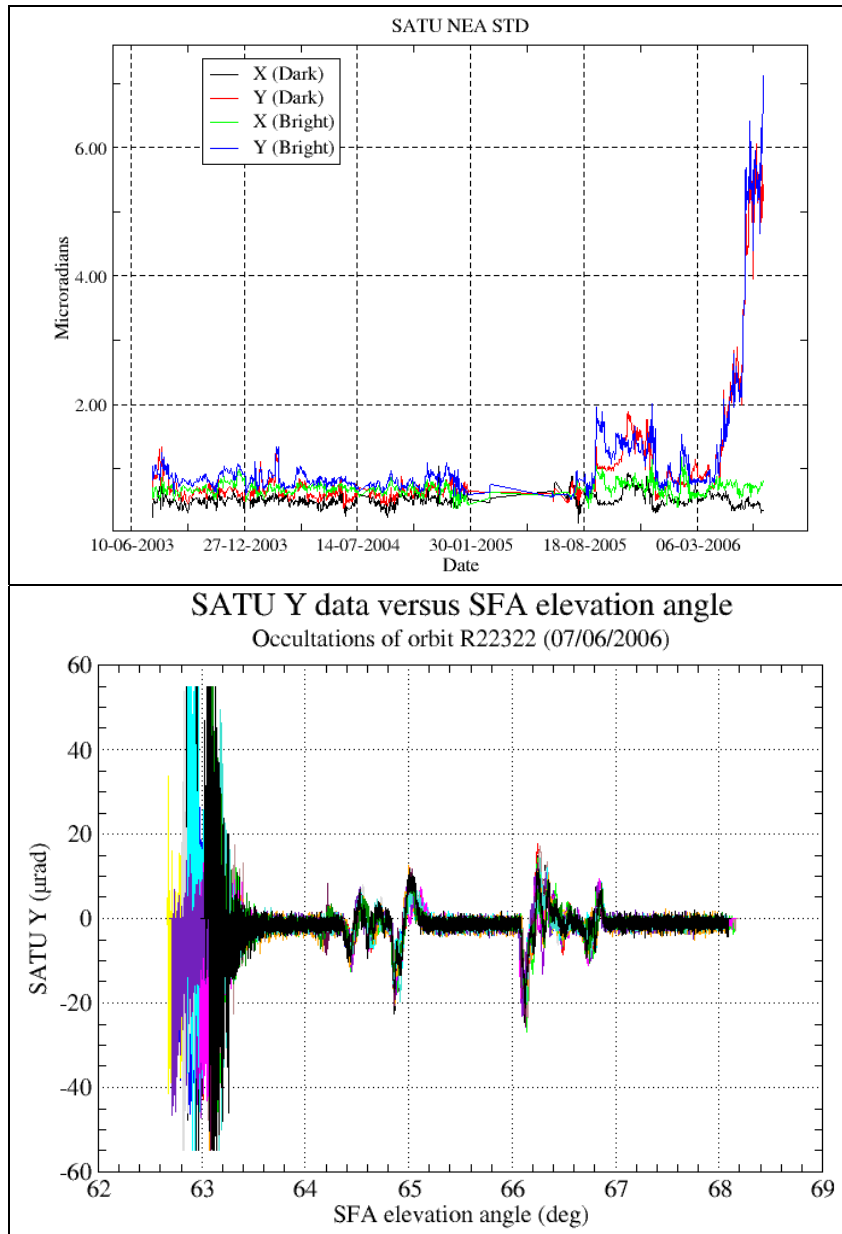
Figure 4.6-1: (Upper plot) Average value per day of SATU NEA STD above 105 km.
(Lower plot) SATU 'Y' data as a function of elevation angle

The results for some occultations belonging to previous months (monthly averages) are presented in fig. 4.6-2, where the change in trend in September 2005 and May 2006, mainly for the 'Y' axis is visible.
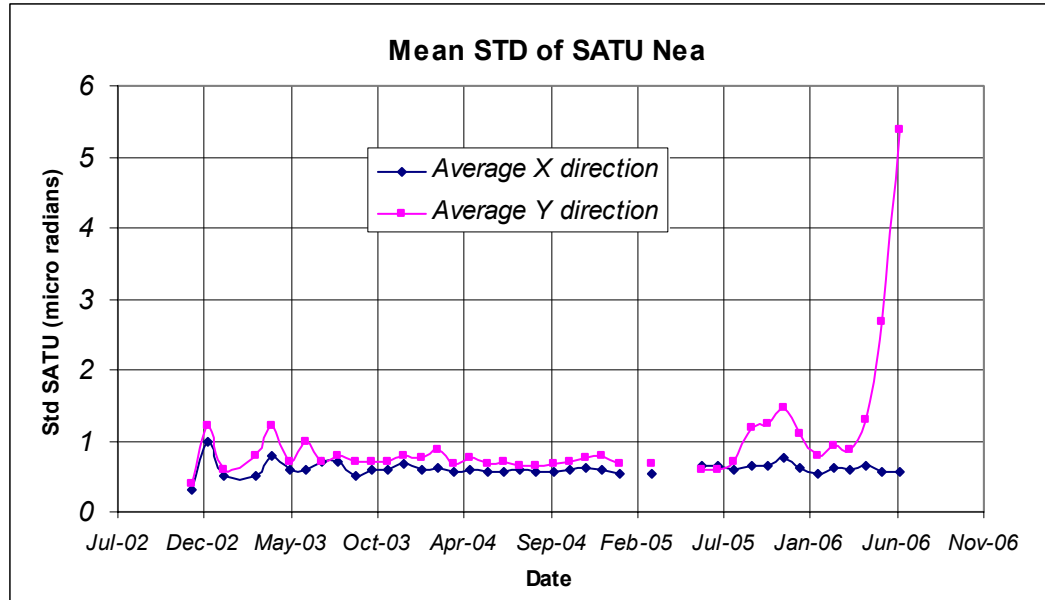
Figure 4.6-2: Average value per month of SATU NEA STD above 105 km

4.6.2 TRACKING LOSS INFORMATION

This verification consists of the monitoring of the tangent altitude at which the star is lost. It is an indicator of the pointing performance although it is to be considered that star tracking is also lost due to the presence of clouds and hence not only due to deficiencies in the pointing performance. Therefore, only the detection of any systematic long-term trend is the main purpose of this monitoring. The recent results are presented in fig. 4.6-3 and 4.6-4:

- The dependence of the altitude at which tracking is lost on the magnitude of the star is very small because the tracking is mainly lost due to the refraction and the scintillation that depend on the atmospheric conditions.
- The azimuth of some stars could be very near to the reduced instrument azimuth edges and therefore there could be occultations planned to have a duration very small (2, 6, 10…seconds).To avoid planning this kind of useless occultation, it has been decided to set the minimum occultation duration value to 25 seconds. Fig. 4.6-3 and 4.6-4 (dark and bright limb) shows stars lost at altitudes higher than 30 km which corresponds with durations around 25-35 seconds.
- In bright limb it is not expected that the stars are lost at very low altitudes due to the amount of light arriving to the pointing system mainly when the refraction effects start to be important. We see from fig. 4.6-4 that there are few stars lost at altitudes around 4 km. This occurs when the pointing system is not able to point to the star anymore but, instead of finishing the occultation, it continues to track light until the planned duration is reached.
- Daily statistics are given in fig. 4.6-5 (calculated using 50 products per day). The high peaks in standard deviation before 25th January 2005 are due to the long lasting occultations or partial occultations (the entire occultation is included within the following orbit data). The ones during June/July/August 2005 are due to the tests performed for the anomaly investigation. After 29th August (GOMOS operational again) the peaks are due to the "short occultations".

- Monthly statistics are given in fig. 4.6-6 (calculated using 50 products per day) where the change in trends, mainly for dark limb, is visible for the period of GOMOS testing.
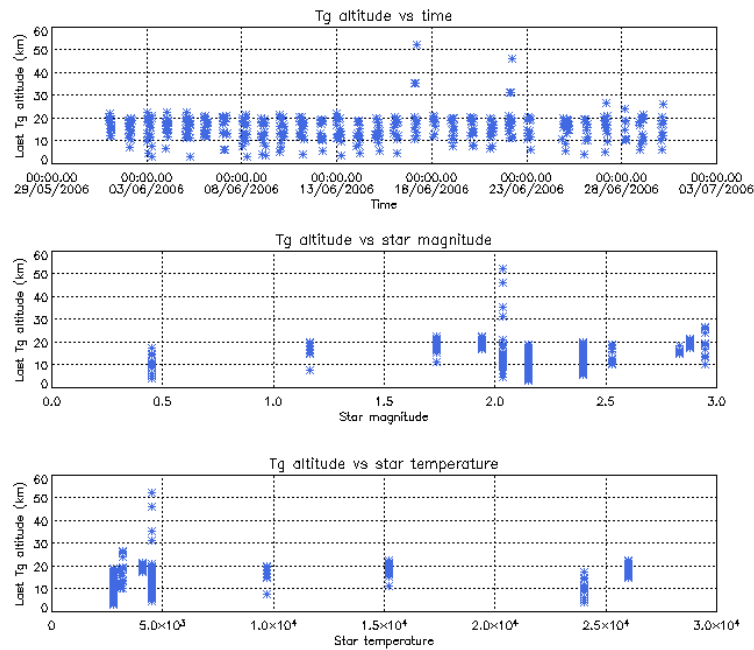

Figure 4.6-3: Last tangent altitude of the occultation (dark limb), point at which the star is lost
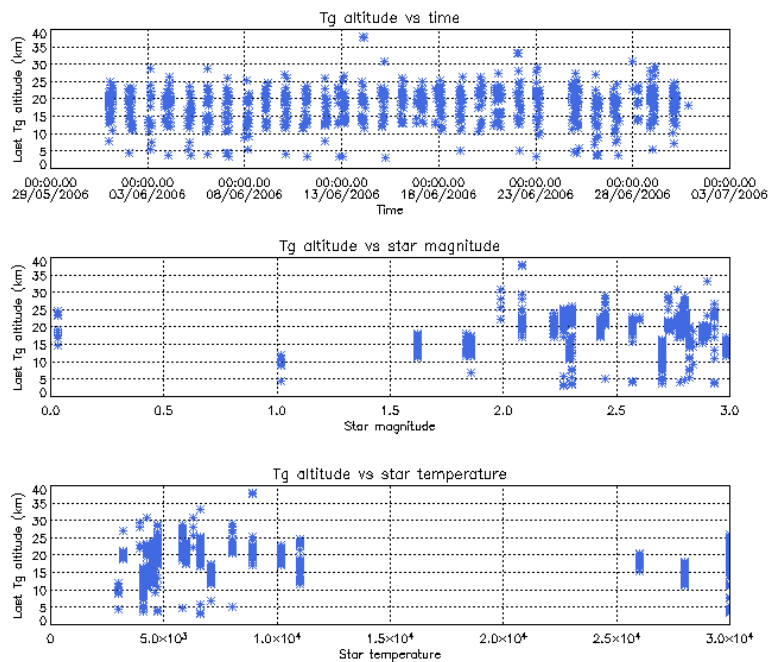

Figure 4.6-4: Last tangent altitude of the occultation (bright limb), point at which the star is lost
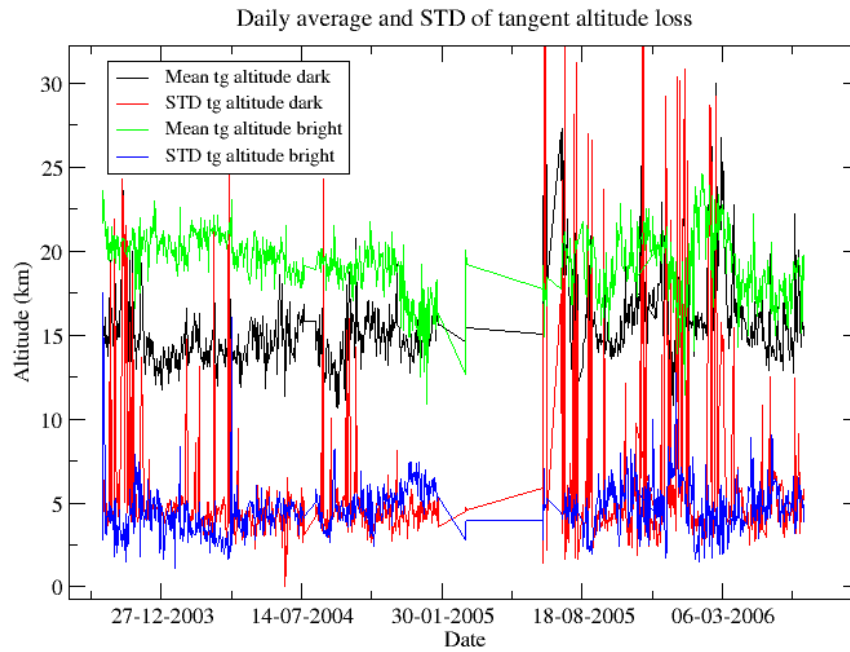
29

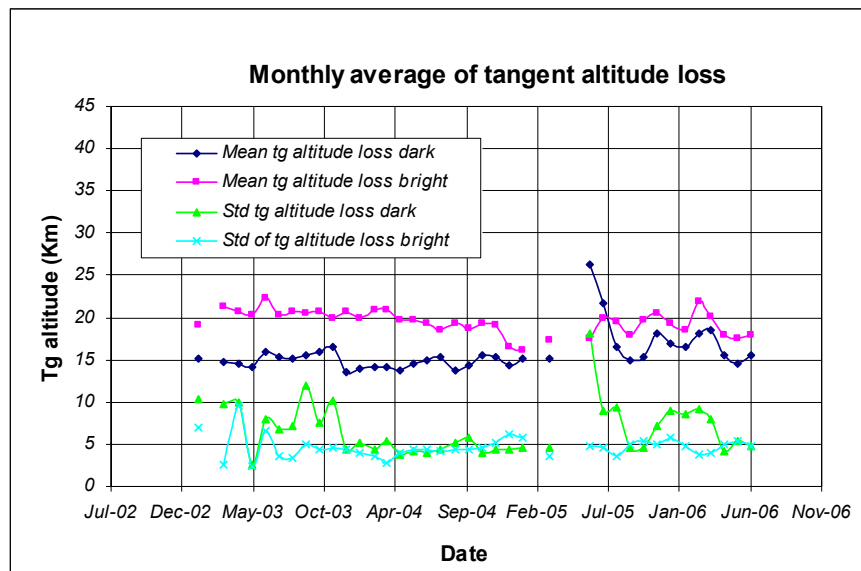**Figure 4.6-5: Daily average and STD of tangent altitude loss for the reporting period**

Figure 4.6-6: Monthly mean tangent altitude (and STD) at which the star is lost since January 2003

4.6.3 MOST ILLUMINATED PIXEL (MIP)

The MIP (Most Illuminated Pixel) is the star position on the SATU CCD in detection mode and it is recorded in the housekeeping data. The nominal centre of the SATU is pixel number **145** in elevation and number **205** in azimuth. The detection of the stars should not be far from this centre. As it can be seen in fig. 4.6-7 the **azimuth MIP** was within the threshold (table 4.6-1) since September 2002 until the occurrence of the anomaly on January 2005, even if a small variation is present. The reason for the change in trend observed after the anomaly is, at the moment, not understood. The **elevation MIP** had a significant variation (see the _note_ below) until 12th December 2003 when a new PSO algorithm was activated in order to reduce the deviations of the ENVISAT platform attitude with respect to the nominal one. Similarly to the azimuth, after the anomaly of January 2005 the Elevation MIP has a drift that has no explanation. Investigations are ongoing to try to understand this behavior of the MIP as, although it does not impact the data quality or the star location on the CCD array during the measurements, it may invalidate attitude monitoring by GOMOS and could represent a hidden anomaly.

Note: A MIP variation onto the SATU CCD of 50 pixels corresponds to a de-pointing of 0.1 degrees

Table 4.6-1: MIP Thresholds

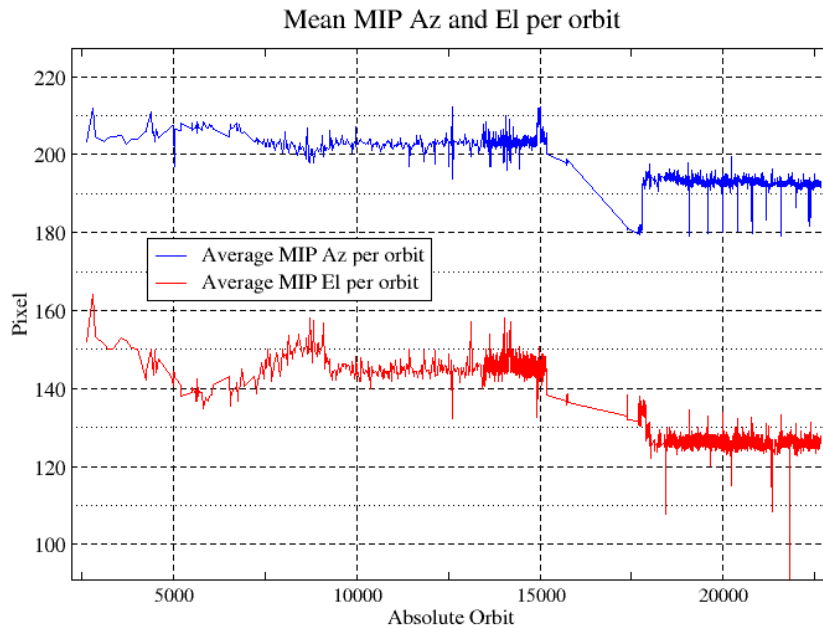| MIP X	Mean delta Az	[198 - 210]
	Std delta Az	7
MIP Y	Mean delta El	[140 – 150]
	Std delta El	4

Figure 4.6-7: Mean values of MIP for some orbits since 1st September 2002 (see table 4.6-1)

31

Fig. 4.6-8 shows the standard deviation of azimuth and elevation MIP that should be within the thresholds of table 4.6-1. The peaks observed mean that one (or more) stars were detected very far from the SATU detection point and, in this case, the stars were lost during the centering phase (see section 3.2 for stars lost in centering).
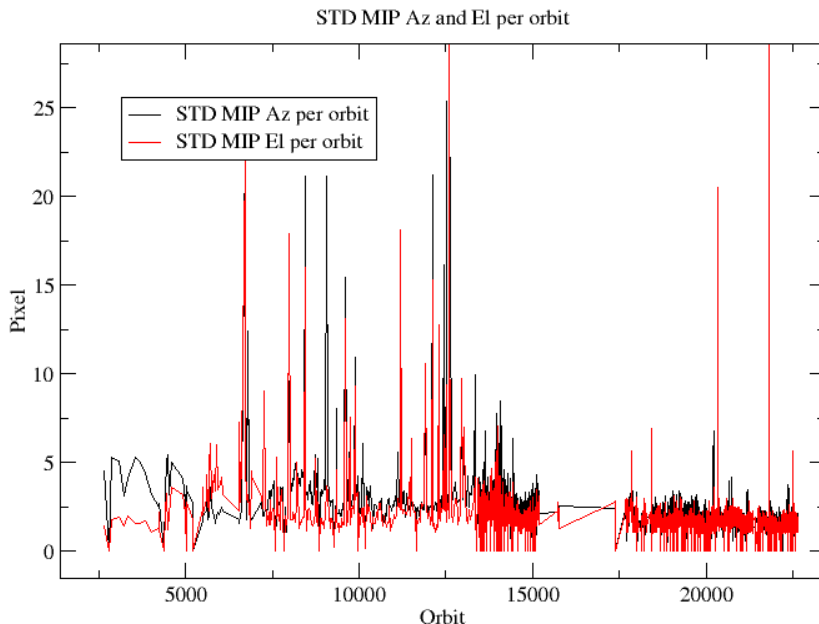

Figure 4.6-8: Standard deviation of MIP Azimuth and Elevation for some orbits since 1st September 2002 until end of reporting period (see table 4.6-1)

5   LEVEL 1 PRODUCT QUALITY MONITORING

5.1   *Processor Configuration*

5.1.1 VERSION

About 21% of near real time GOM_TRA_1P products have been received by the DPQC team for routine quality control and long term trend quality monitoring. The current level 1-processor software version for the operational ground segment is GOMOS/4.02 (see table 5.1-1). The product specification is PO-RS-MDA-GS2009_10_3H. This processor has been cleared for initial level 1 data release, with a disclaimer for known artefacts (http://envisat.esa.int/dataproducts/availability/disclaimers) that are currently being resolved and will be implemented in the next release (http://envisat.esa.int/dataproducts/availability).

Users are supplied with 2002-2005 and beginning of 2006 (until March) data sets reprocessed by the last prototype processor GOPR_6.0c_6.0f developed and operated by ACRI. See table 5.1-2 for prototype level 1b versions and modifications. The next GOMOS operational ground segment version (GOMOS/5.00) will be in line with the prototype version used for this second reprocessing.

Table 5.1-1: PDS level 1b product version and main modifications implemented

Date	Version	Description of changes
23-MAR-2004	Level 1b version 4.02 at PDHS-E and PDHS-K	Algorithm baseline level 1b DPM 6.0 • Adding a new calibration parameters (these values are hard coded at the moment) • Removal of redundancy chain from code • Modifications in the processing to apply new configuration and calibration parameter • New algorithm to determine between dark, twilight and bright limb and to handle data accordingly • Added handling of source packages with invalid packet header • Added enumerations for all configuration flags
31-MAY-2003	Level 1b version 4.00 at PDHS-E and PDHS-K	Algorithm baseline level 1b DPM 5.4: • Modulation correction step added after the cosmic rays detection processing • Inversion of the non-linearity and offset corrections • Modification of the computation of the estimated background signal measured by the photometers: use the spectrometer radiometric sensitivity curve and the photometer transfer function. • Use of the dark charge map at orbit level computed from the DSA (dark sky area) if any in the level 0 product • Implementation of a new unfolding algorithm for the photometer samples
21-NOV-2002	Level 1b version 3.61 at PDHS-E and PDHS-K	Algorithm baseline DPM 5.3: • Review of some default values • New definition of one PCD flag (atmosphere) • Temporal interpolation of ECMWF data

Table 5.1-2: GOPR level 1b product version and main modifications implemented

Date	Version	Description of changes
22-JUL-2005	GOPR_6.0c	Level 1b: • Correction of FP unfolding algorithm • Background correction of SPB in full dark limb • Modification of the computation of the incidence angle • Correction of the flat-field correction equations • Star spectrum location on CCD modified for SPB Configuration for second reprocessing: • Use of new reflectivity LUT • New wavelength assignment for SPA1, A2, B1 • Spatial PSF of SPB modified
17-MAR-2004	GOPR 6.0a	• Provide SFA and SATU angles in degrees • Elevation angle dependency of the reflectivity LUT added in the algorithms • Ratio upper/star signal added (FLAGUC) • Add Dark Charge used for dark charge correction (per band) • Flag for illumination condition (PCDillum) • Minimum sample value for which the cosmic rays detection processing is applied (Crmin) is a function of gain index • Logic for computation of the flags attached to the reference star spectrum

		(Flref) modified • Add the computation of the sun direction in the inertial geocentric frame to be written in the level 1b and limb products. • Spectrometer effective sampling time added
25-JUL-2003	GOPR 5.4f	• The demodulation process is applied only in full dark limb and twilight limb conditions.
17-JUL-2003	GOPR 5.4e	• Sun zenith angle is computed in the geolocation process. The occultation is now classified into (0) full dark limb condition, (1) bright limb condition and (2) twilight limb condition. • No background correction applied in full dark limb condition. The location of the image of the star spectrum on the CCD array is no more aligned with the CCD lines.
02-JUL2003	GOPR 5.4d	• The maximum number of measurements is set to 509 (instead of 510) in the GOPR prototype.
17-MAR-2003	GOPR 5.4c	• Modification of the CAL ADFs (update of the limb radiometric LUT). The products are affected only if the limb spectra are converted into physical units • Modifications to allow compatibility with ACRI computational cluster (no modifications of the results) • Modification of the logic to handle dark charge map refresh at orbit level (DSA data is now directly processed by the level 1b processor if available in the level 0 product). No impact on the results
21-FEB-2003	GOPR 5.4b	• DC map values are rounded when written in the level 1b product • Modification of the CAL ADFs (update of the wavelength assignment of SPB1 and SPB2) • Modify the computation of flag_mod in the modulation correction routine
17-JAN-2003	GOPR 5.4a	• use the start and stop dates of the occultation when calling the CFI nterpol instead of start and stop dates of the level 0 product • modify the ECMWF filename information in the SPH of the level 1b and limb products

5.1.2 AUXILIARY DATA FILES (ADF)

The ADF's files in tables 5.1-3, 5.1-4, 5.1-5, 5.1-6 and 5.1-7 have been disseminated to the PDS during the whole mission. Note that the files outlined in yellow are the set of auxiliary files used during the reporting period. For every type of file, the validity runs from the start validity time until the start validity time of the following one, but if an ADF file has been disseminated after the start validity time, it is obvious that it will be used by the PDHS-E and PDHS-K PDS only after the dissemination time (this happens the majority of the time). Just like the other ADF's, the calibration auxiliary file (GOM_CAL_AX) has been updated several times in the past (table 5.1-7) but the difference is that now it is updated in a weekly basis with only new DC maps, and that is why the files used during May 2006 are reported in a separate table (table 5.1-8) that changes from report to report.

Table 5.1-3: Table of historic GOM_PR1_AX files used by PDS for level 1b products generation. The GOM_PR1_AX is a file containing the configuration parameters used for processing from level 0 to level 1b products

Used by PDS for Level 1b products generation in period	GOM_PR1_AX (GOMOS processing level 1b configuration file)
01-MAR-2002 → 29-MAR-2002	**GOM_PR1_AXVIEC20020121_165314_20020101_000000_20200101_000000** • Pre-launch configuration
30-MAR-2002 → 14-NOV-2002	**GOM_PR1_AXVIEC20020329_115921_20020324_200000_20100101_000000** • Changed num_grid_upper, thr_conv and max_iter in the atmospheric GADS
Not used	**GOM_PR1_AXVIEC20020729_083756_20020301_000000_20100101_000000** • Cosmic Ray mode + threshold • DC correction based on maps • Non-linearity correction disabled
Not used	**GOM_PR1_AXVIEC20021112_170331_20020301_000000_20100101_000000** • Central background estimation by linear interpolation + associated thresholds
15-NOV-2002 → 26-MAR-2003	**GOM_PR1_AXVIEC20021114_153119_20020324_000000_20100101_000000** • Same content as GOM_PR1_AXVIEC20021112_170331_20020301_000000_20100101_000000 but validity start updated so as to supersede according to the PDS file selection rules GOM_PR1_AXVIEC20020329_115921_20020324_200000_20100101_000000
27-MAR-2003 → 19-MAR-2004	**GOM_PR1_AXVIEC20030326_085805_20020324_200000_20100101_000000** • Same content as GOM_PR1_AXVIEC20021112_170331_20020301_000000_20100101_000000 but validity start updated so as to supersede according to the PDS file selection rules GOM_PR1_AXVIEC20020329_115921_20020324_200000_20100101_000000
20-MAR-2004 → 22-MAR-2004	**GOM_PR1_AXVIEC20040319_134932_20020324_200000_20100101_000000** • Ray tracing parameter changed: convergence criteria set to 0.1 microrad
23-MAR-2004 → 01-APR-2004 *Notes*: • This file was constructed from GOM_PR1_AXVIEC20030326_085805_20020324_200000_20100101_000000 (so without the ray tracing parameter changed) • This file was used by the GOMOS/4.02 processors before the IECF dissemination. The dissemination was done on 25th March 2004	**GOM_PR1_AXVIEC20040316_144850_20020324_200000_20100101_000000** GOM_PR1 ADF for version GOMOS/4.02, changes: • The central band estimation mode • Atmosphere thickness • Altitude discretisation
02-APR-2004	**GOM_PR1_AXVIEC20040401_083133_20020324_200000_20100101_000000** • Ray tracing parameter changed: convergence criteria set to 0.1 microrad

Table 5.1-4: Table of historic GOM_INS_AX files used by PDS for level 1b products generation. The GOM_INS_AX is a file containing the characteristics of the instrument and it is used for processing from level 0 to level 1b products and from level 1b to level 2 products

Used by PDS for Level 1b products generation in period	GOM_INS_AX (GOMOS instrument characteristics file)
01-MAR-2002 → 29-JUL-2002	GOM_INS_AXVIEC20020121_165107_20020101_000000_20200101_000000 • Pre-launch configuration
30-JUL-2002 → 12-NOV-2002	GOM_INS_AXVIEC20020729_083625_20020301_000000_20100101_000000 • Factors for the conversion of the SFA angles from SFM axes to GOMOS axes
13-NOV-2002 → 16-JUL-2003	GOM_INS_AXVIEC20021112_170146_20020301_000000_20100101_000000 • No more invalid spectral range
Not used	GOM_INS_AXVIEC20030716_080112_20030711_120000_20100101_000000 • New value for SFM elevation zero offset for redundant chain: 10004
17-JUL-2003	GOM_INS_AXVIEC20030716_105425_20030716_120000_20100101_000000 • Bias induct azimuth redundant value set to -0.0084 rad (-0.4813 deg)

Table 5.1-5: Table of historic GOM_CAT_AX files used by PDS for level 1b products generation. The GOM_CAT_AX is a file holding the star catalogue used for processing from level 0 to level 1b products

Used by PDS for Level 1b products generation in period	GOM_CAT_AX (GOMOS Stat Catalogue file)
01-MAR-2002	GOM_CAT_AXVIEC20020121_161009_20020101_000000_20200101_000000 • Pre-launch configuration

Table 5.1-6: Table of historic GOM_STS_AX files used by PDS for level 1b products generation. The GOM_STS_AX is a file containing star spectra used for processing from level 0 to level 1b products

Used by PDS for Level 1b products generation in period	GOM_STS_AX (GOMOS Star Spectra file)
01-MAR-2002	GOM_STS_AXVIEC20020121_165822_20020101_000000_20200101_000000 • Pre-launch configuration

Table 5.1-7: Table of historic GOM_CAL_AX files used by PDS for level 1b products generation. The GOM_CAL_AX is a file containing the calibration parameters used for processing from level 0 to level 1b products

Used by PDS for Level 1b products generation in period	GOM_CAL_AX (GOMOS Calibration file)
01-MAR-2002 → 29-JUL-2002	GOM_CAL_AXVIEC20020121_164808_20020101_000000_20200101_000000 • Pre-launch configuration
Not used	GOM_CAL_AXVIEC20020121_142519_20020101_000000_20200101_000000 • Pre-launch configuration
30-JUL-2002 → 12-NOV-2002	GOM_CAL_AXVIEC20020729_082426_20020717_193500_20100101_000000 • Band setting information • Wavelength assignment • Spectral dispersion LUT • ADC offset for Spectrometers • PRNU maps • Thermistor coding LUT • DC maps

Not used	**GOM_CAL_AXVIEC20021112_165603_20020914_000000_20100101_000000** • Band setting information • DC maps • PRNU maps • Wavelength assignment • Spectral dispersion LUT • Radiometric sensitivity LUT (star and limb) • SP-FP intercalibration LUT • Vignetting LUT • Reflectivity LUT • ADC offset
13-NOV-2002 → 30-JAN-2003	**GOM_CAL_AXVIEC20021112_165948_20021019_000000_20100101_000000** • Only DC maps updated
31-JAN-2003 → 11-APR-2003	**GOM_CAL_AXVIEC20030130_133032_20030101_000000_20100101_000000** • Only DC maps updated (using DSA of orbit 04541)
12-APR-2003 → 02-JUN-2003	**GOM_CAL_AXVIEC20030411_065739_20030407_000000_20100101_000000** • Modification of the radiometric sensitivity curve for the limb spectra. Note that the modification of this LUT has no impact on the GOMOS processing. The LUT is just copied into the level 1b limb product for user conversion purpose. • Updated DC map only (using DSA of orbit 05762).
03-JUN-2003: from this date onwards, mainly updates to DC maps are done. Every month, the table of new GOM_CAL files with **only** DC maps updated is provided (table 5.1-8). Eventual changes to this file not corresponding only to DC maps updates will be reported in this table.	**GOM_CAL_AXVIEC20030602_094748_20030531_000000_20100101_000000** • Updated DC maps only (using DSA of orbit 06530)
13-FEB-2004 → 23-FEB-2004	**GOM_CAL_AXVIEC20040212_103916_20040209_000000_20100101_000000** • Update of the reflectivity LUT • Updated DC maps (Orbit 10194, date 11-FEB-2004)

Table 5.1-8: Calibration ADF for reporting period. These files are updated (only with DC maps) in a 8-10 days basis

Used by PDS for Level 1b products generation in period	GOM_CAL_AX (GOMOS Calibration file)
30-MAY-2006 → 12-JUN-2006	**GOM_CAL_AXVIEC20060529_110511_20060527_000000_20100101_000000** (orbit 22178, date 28 MAY 2006)
13-JUN-2006 → 21-JUN-2006	**GOM_CAL_AXVIEC20060612_084204_20060610_000000_20100101_000000** (orbit 22377, date 11 JUN 2006)
22-JUN-2006 → 29-JUN-2006	**GOM_CAL_AXVIEC20060621_093306_20060619_000000_20100101_000000** (orbit 22508, date 20 JUN 2006)
30-JUN-2006	**GOM_CAL_AXVIEC20060629_085700_20060627_000000_20100101_000000** (orbit 22627, date 28 JUN 2006)

5.2   Quality Flags Monitoring

In this section, the results of monitoring some Product Quality information stored in level 1b products that did not have a fatal error (MPH error flag not set) are discussed. The products with fatal errors were around 0.3% of the products received during the reporting month for the quality monitoring.

On the one hand, for every product we have information of the **number of measurements** where a given problem was detected (i.e. number of invalid measurements, number of measurements containing saturated samples, number of measurements with demodulation flag set…). On the other hand, there are **flags** that indicate problems within the product (i.e. flag set to one if the reference spectrum was computed from DB, flag set to zero if SATU data were not used…).

For the information on the number of measurements a plot of percentages with respect to time is provided in fig. 5.2-1. The most relevant part of this information is also plotted in a world map as a function of ENVISAT position: % of cosmic ray hits per profile, % of datation errors per profile, % of star falling outside the central band per profile and % of saturation errors per profile (fig.5-2.2).

It can be seen from fig. 5.2-1 that the cosmic rays hits occurred several times for the 95% of the measurements of the products. Looking at fig. 5.2-2 it can be clearly observed that this high percentage occurred when the satellite crossed the South Atlantic Anomaly (SAA) zone. The percentage of saturation errors per profile shows a slight increase over the SAA zone.

Another observation from fig. 5.2-1 is that for many products, 20-25% of the measurements have the star signal falling outside the central band. In fig. 5.2-2 it is observed that this percentage occurred mainly during the ascending part of the orbit (twilight/night-side of the orbit) while in the descending part (day-side of the orbit) the percentage is around 10%. This is because during the night the stars are lost deeper within the atmosphere and the turbulence phenomena becomes more important, producing the star to be less 'focused' on the spectrometers central band.
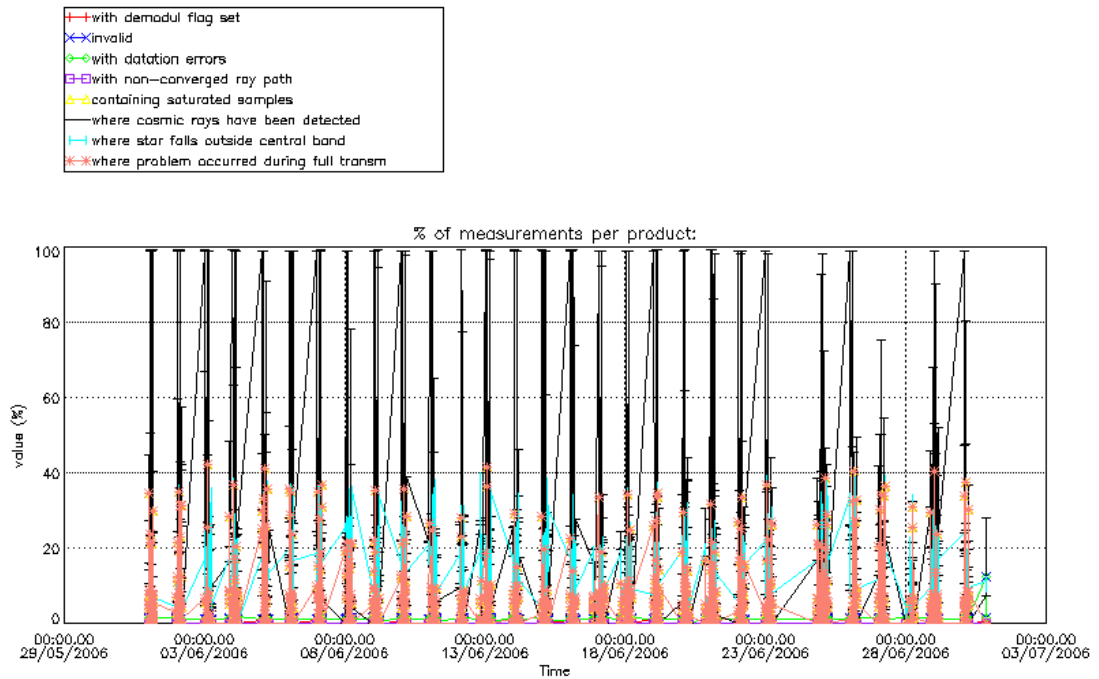
Figure 5.2-1: Level 1b product quality monitoring with respect to time
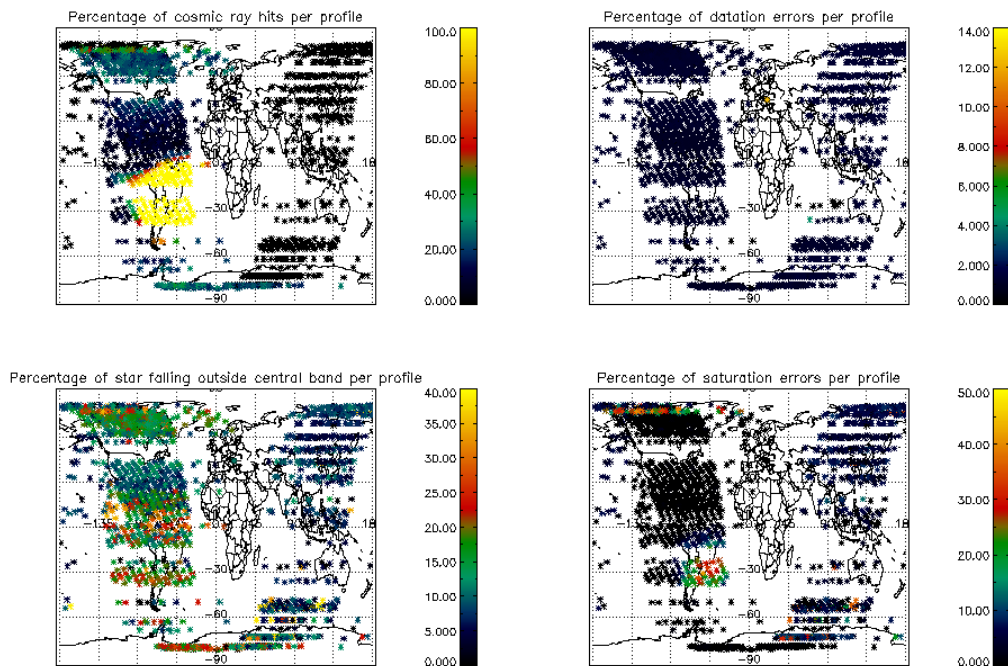

Figure 5.2-2: Level 1b product quality monitoring with respect to geolocation of ENVISAT

The other values (% of invalid measurements per product, % of measurements per product with datation errors…) are quite low.

The flag information is given in table 5.2-1. The percentage of the products that have at least one measurement with demodulation flag set is also reported.

Table 5.2-1: Percentage of products during the reporting period with:

At least one measurement with demodulation flag set:	12 %
Reference spectrum computed from DB:	0.0 %
Reference spectrum with small number of measurements:	0.0 %
SATU data not used:	0.0 %

5.2.1 QUALITY FLAGS MONITORING (EXTRACTED FROM LEVEL 2 PRODUCTS)

In this section, the Product Quality information coming from the level 1 processing that is also stored in the level 2 products is plotted. Only products that did not have a fatal error (MPH error flag not set) are considered. The purpose of using the level 2 data is simply that the percentage of level 2 products arriving to the DPQC team for the quality monitoring is much higher. For the reporting month, 84% of the archived products have been received. The plots are very similar to fig. 5.2-1 and 5.2-2 (demodulation flag information is not included) but separating ascending from descending passes (see table 5.2-2). Fig. 5.2-3 and 5.2-4 present some quality information as a function of the time whereas in fig. 5.2-5 and 5.2-6 the plot is respect to the satellite position at the beginning of the occultations.

Table 5.2-2: Latitude of the different limb illumination in ascending and descending passes

Ascending	**Dark:** [-70°, 30°] **Twilight:** below -80° , [35° - 45°] **Bright:** above 55°
Descending	**Dark:** No **Twilight:** below -70° **Bright:** above -65°

In ascending (fig. 5.2-3) the percentage of measurements "where a problem occurred during the full transmission" per product is around 2% while for the descending passes (fig. 5.2-4) is around 10%. This is due to the saturation that occurs mainly in bright limb. In ascending the saturation occurs over the SAA zone but it is quite low elsewhere. From fig. 5.2-3 (twilight/night-side of the orbit) you can see also that, for many products, 25-30 % of the measurements have the star signal falling outside the central band. In the descending part (day-side of the orbit) the percentage is around 10-15 % (fig. 5.2-4). This is because during the night the stars are lost deeper within the atmosphere and the turbulence phenomena become more important, resulting in the star being less 'focused' on the spectrometers central band.

In ascending (fig. 5.2-5) the SAA is perfectly localized by the high percentage of cosmic ray hits per product (upper left panel). It is not the same if we look at fig. 5.2-6, because in descending most of the

occultations are in bright limb conditions (see table 5.2-2) and the cosmic rays detection processing is not activated.
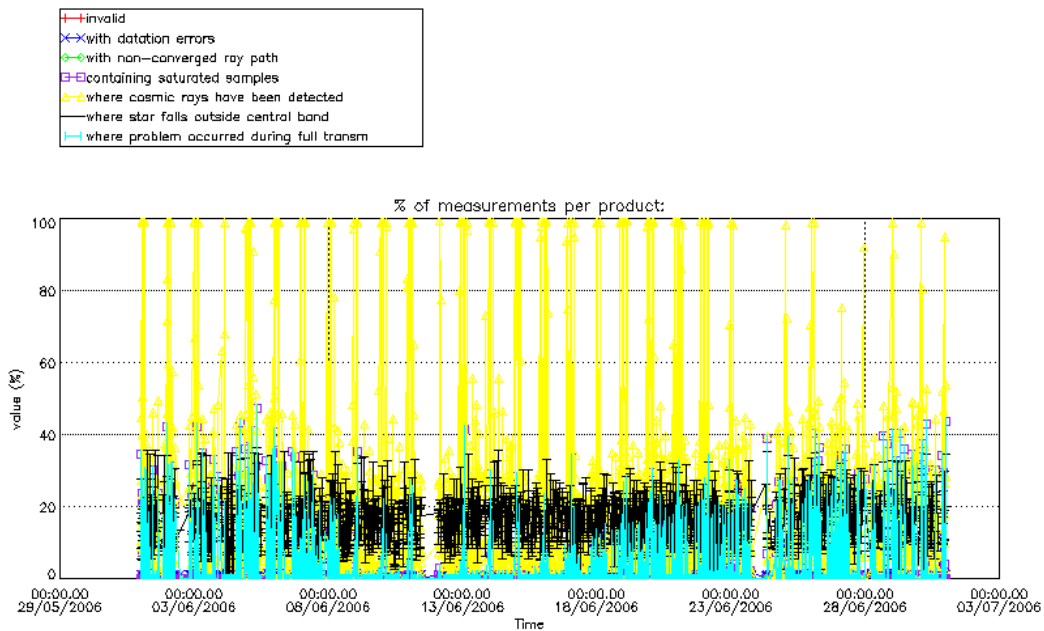

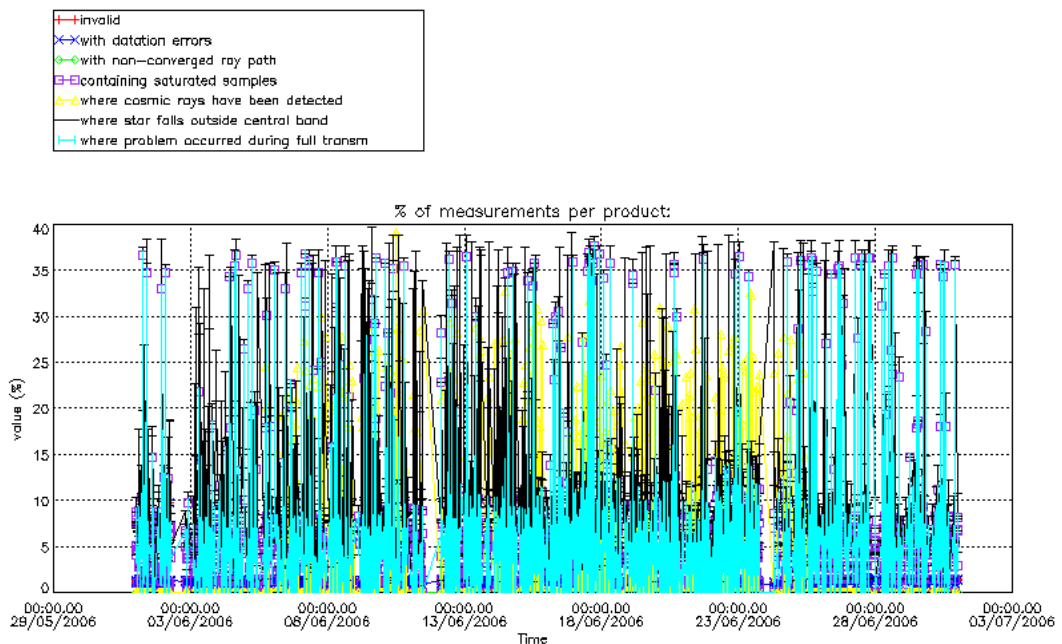**Figure 5.2-3: Level 1b product quality monitoring with respect to time <u>ASCENDING</u> ENVISAT passes**

Figure 5.2-4: Level 1b product quality monitoring with respect to time <u>DESCENDING</u> ENVISAT passes
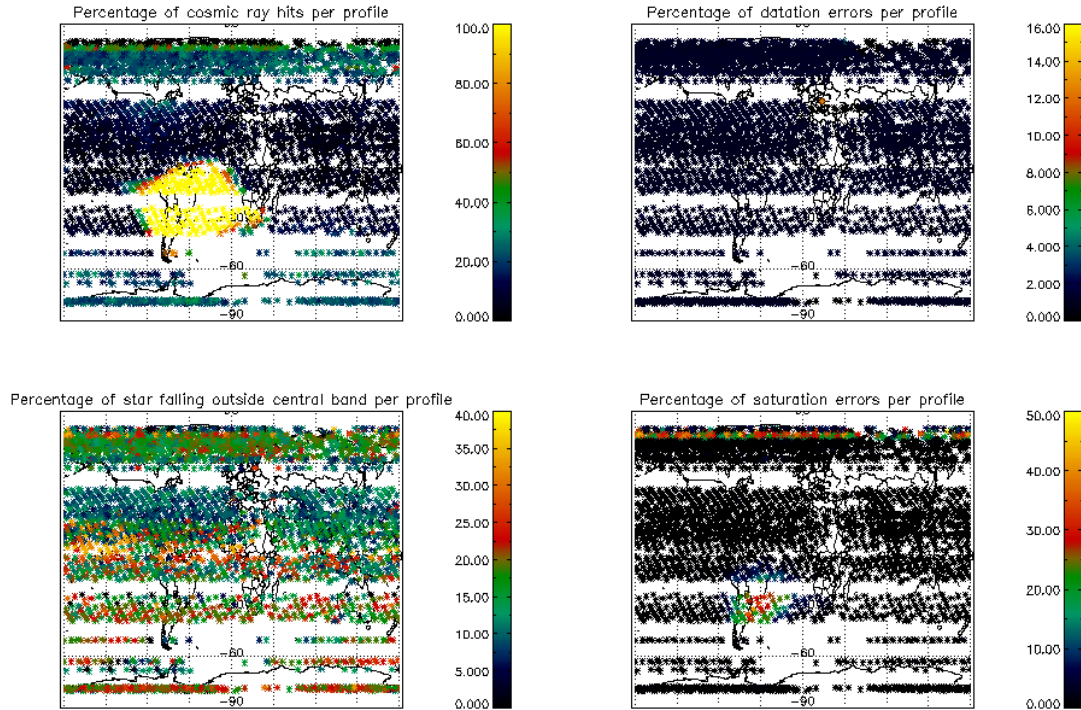
Figure 5.2-5: Level 1b product quality monitoring with respect to geo-location for <u>ASCENDING</u> ENVISAT passes
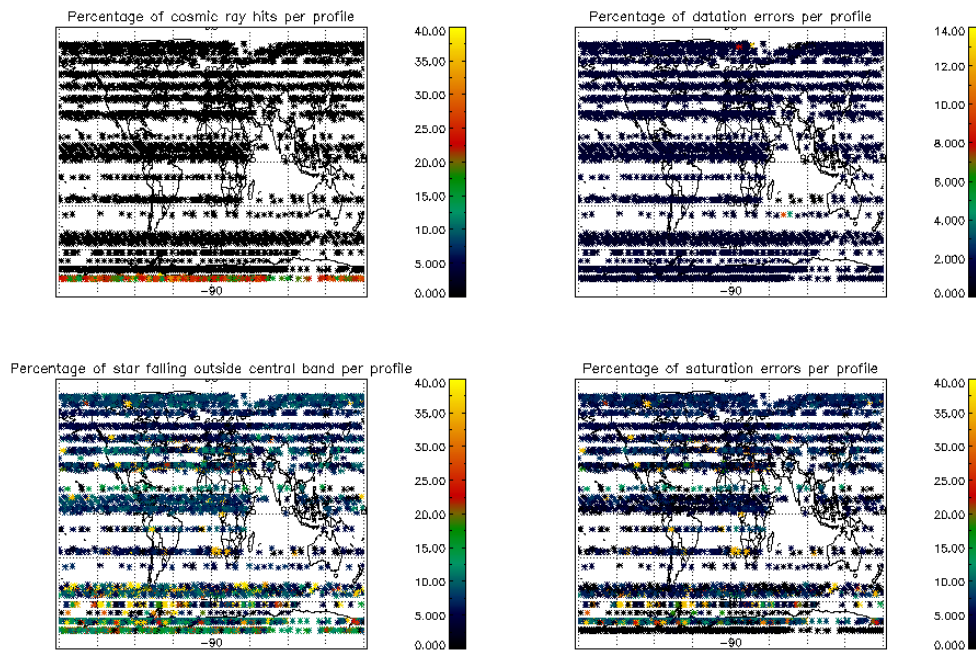

Figure 5.2-6: Level 1b product quality monitoring with respect to geo-location for <u>DESCENDING</u> ENVISAT passes

42

5.3   Spectral Performance

Some spectral calibration exercises have been performed during the reporting period. In previous exercises the results exceeded the warning value which is 0.07 nm (fig. 5.3-1).
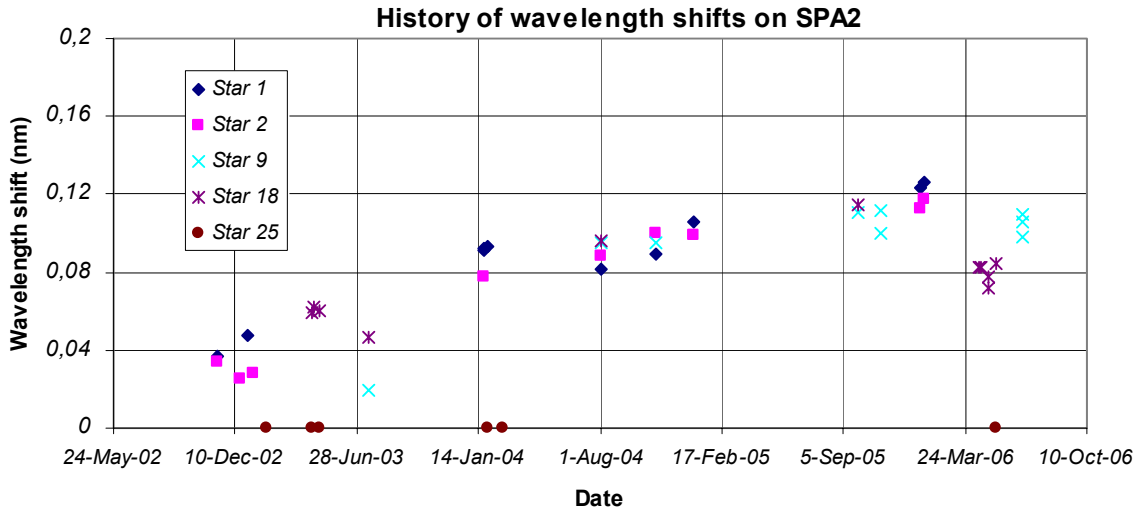

Figure 5.3-1: Wavelength shifts on SPA2 since 12th November 2002 calculated using different stars

The values reported in the plot of fig. 5.3-1 are, for every star ID (1, 2, 9, 18, 25), the spectral shift on SPA2 CCD for which a maximum correlation has been found between the reference spectrum and the one of the occultation.

During the last wavelength calibration analysis performed using some occultations of star id 18 and 9 measured during May/June, the spectral shifts were decreasing again although an increase is expected due to the temperature increase. This effect could be related with the stars themselves and the period of the year (straylight) because they have shown a similar behavior in the past, i.e. May/June 2003.

5.4   Radiometric Performance

5.4.1 RADIOMETRIC SENSITIVITY

The monitoring performed consists of the calculation of the radiometric sensitivity of each CCD by computing the ratio between parts of the reference spectrum using specific stars (fig. 5.4-1). The parts of the spectrum used are:

- UV: 250–300 nm
- Yellow: 500–550 nm
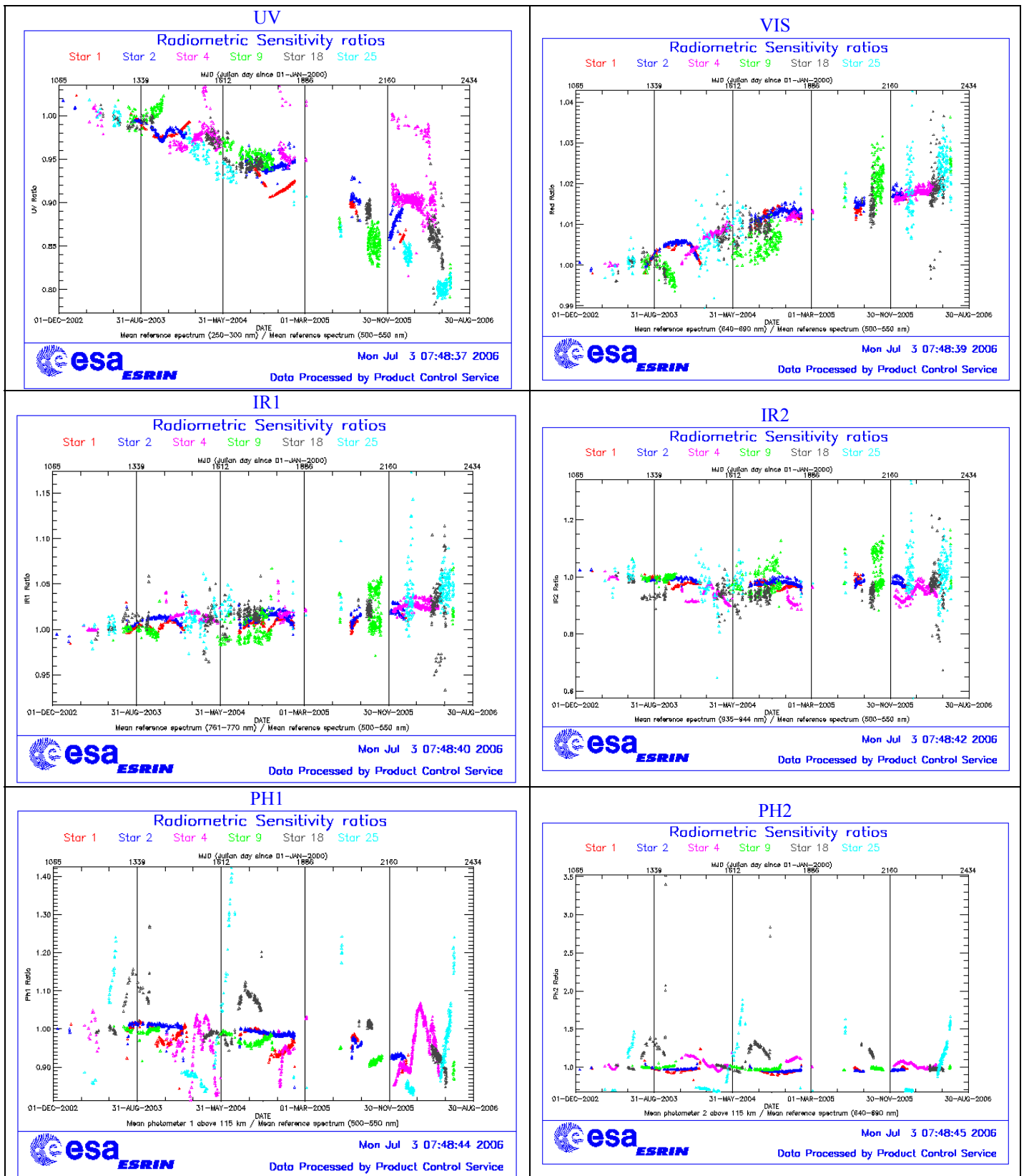- Red: 640–690 nm
- Ir1: 761-770 nm
- Ir2: 935-944 nm

43

Figure 5.4-1: Radiometric sensitivity ratios since December 2002

For the spectrometers the ratios are with respect to the 'yellow' spectral range. For the photometers, the ratios are calculated by dividing the mean photometer signal above the atmosphere (115 km) by the 'yellow' spectral range (for PH1) or by the 'red' spectral range (for PH2).

The variation of the ratio should be within a given threshold which is set to 10% (see table 5.4-1 that corresponds to fig. 5.4-1). For every star, this variation is calculated as the difference between the maximum (or minimum) ratio, and the mean over the 15 first values (if there were not 15 values computed yet, all values would be used).

Table 5.4-1: Variation of RS for the different ratios (corresponds to fig. 5.4-1). Should be less than 10%

Star Id	% Variation of UV ratio	% Variation of Red ratio	% Variation of IR1 ratio	% Variation of IR2 ratio	% Variation of Ph1 ratio	% Variation of Ph2 ratio
1	3.15076	0.605267	0.401701	0.250543	8.55029	30.1656
2	0.810235	0.850594	0.625175	0.383392	8.27717	7.93166
4	0.460608	1.30408	1.52463	1.30163	8.08780	23.5227
9	15.6189	1.21324	0.799394	0.603875	7.61944	9.05862
18	3.17715	1.41829	1.63441	1.76815	14.7885	299.989
25	29.2673	1.35252	1.85261	1.35782	28.0870	147.396

For star 9 and 25 the UV ratio is greater than the threshold 10%. It is clear (fig. 5.4-1) that there is a global decrease of UV ratios for all the stars. This confirms the expected degradation suffered by the UV optics that is, anyway, very small considering also the small variation for the rest of the stars (table 5.4-1).

By looking at the photometers radiometric sensitivity ratios of fig. 5.4-1, it can be seen that every star has a variation that seems to be annual. The variation is significant for stars 25 and 18. After some investigations performed by the QWG that exclude an inaccurate reflectivity correction LUT, it seems that the PH1/2 radiometric sensitivity variations could come from the fact that the spectrometers and the photometers are not illuminated the same way when the straylight appears (seasonal effect).

5.4.2 PIXEL RESPONSE NON UNIFORMITY

No new PRNU calibration has been performed during the reporting period. This means that the PRNU maps inside the ADF remain as they are without any change for the moment.

5.5 *Other Calibration Results*

Future reports will address other calibration results, when available.

6   LEVEL 2 PRODUCT QUALITY MONITORING

6.1   *Processor Configuration*

6.1.1 VERSION

Level 2 products from the operational ground segment have been disseminated during June 2006 to the users. About 84% of GOM_NL__2P products have been received by the DPQC team for routine quality control and long term trend monitoring. The current level 2-processor software version for the operational ground segment is GOMOS/4.02 (see table 6.1-1). The product specification is PO-RS-MDA-GS2009_10_3H. Users are also supplied with 2002-2005 (and Jan-March 2006) data sets reprocessed by the last prototype processor GOPR_6.0c_6.0f developed and operated by ACRI. The next GOMOS operational ground segment version (GOMOS/5.00) will be in line with the prototype version used for this second reprocessing.

Table 6.1-1: PDS level 2 product version and main modifications implemented

Date	Version	Description of changes
23-MAR-2003	Level 2 version 4.02 at PDHS-E and PDHS-K	Algorithm baseline level 2 DPM 5.5: Section 3 • Add references to technical notes on Tikhonov regularization • Change High level breakdown of modules: SMO/PFG • Change parameter: NFS in l2 ADF • Change parameter σ_G in l2 ADF (Table 3.4.1.1-II) • Change content of Level 2/res products – GAP • Change time sampling discretisation • Add covariance matrix explanation Section 5 • Replace SMO by PFG VER-1/2: Depending on NFS, Apply either a Gaussian filter or a Tikhonov regularization to the vertical inversion matrix • Unit conversion applied on kernel matrix • Suppress VER-3 Section 6 • GOMOS Atmospheric Profile (GAP): not used in this version • Time sampling in equation (6.5.3.7-73)

		Algorithm baseline level 2 DPM 5.4:
31-MAY-2003	Level 2 version 4.00 at PDHS-E and PDHS-K	• Revision of some default values • Add a new parameter • Transmission model computation: suppress tests on valid pixels and species • Apply a Gaussian filter to the vertical inversion matrix • Very low signal values are substituted by threshold value
21-NOV-2002	Level 2 version 3.61 at PDHS-E and PDHS-K	Algorithm baseline level 2 DPM 5.3a: • Revision of some default values • Wording of test T11 • Dilution term computation of jend • Covariance computation scaling applied before and after

Table 6.1-2: GOPR level 2 product version and main modifications implemented

Date	Version	Description of changes

14-OCT-2005	GOPR_6.0f	• The optimisation of the DOAS iterations
		• Negative column densities and local densities not flagged anymore
		• Suppress the setting of maximum error in case of negative local densities
		• Correction of HRTP discrepancies, and error estimates fixed
		Configuration for second reprocessing:
		    • 2nd order polynomial for aerosol
		    • Air fixed to ECMWF (local density set to 0 in the L2 products)
		    • Orphal cross-sections for O_3
		    • GOMOS cross-sections for other species
		    • Covariance matrix terms linked to air set to 0
		    • Air and NO_2 additional errors set to 0

17-MAR-2004	GOPR 6.0a	• Rename Turbulence MDS into High Resolution Temperature MDS (HRTP) • Add vertical resolution per species in local densities MDS • Add Solar zenith angle at tangent point and at satellite level in geolocation ADS • Add "tangent point density from external model" in geolocation ADS • Suppress contribution of "tangent point density from external model" in "local air density from GOMOS atmospheric profile" in geolocation ADS
18-AUG-2003	GOPR 5.4d	• Tikhonov regularisation is implemented
18-MAR-2003	GOPR 5.4b	• Modification to implement the computation of Tmodel for spectrometer B (in version 5.4b, the Tmodel for SPB is still set to 1)
30-JAN-2003	GOPR 5.4a	• Modifications for ACRI internal use only. No impact on level 2 products.

6.1.2 AUXILIARY DATA FILES (ADF)

The ADF's files in table 6.1-3 and 6.1-4 are used by the PDS to process the data from level 1 to level 2. For every type of file, the validity runs from the start validity time until the start validity time of the following one, but if an ADF file has been disseminated after the start validity time, it is obvious that it will be used by the PDHS-E and PDHS-K PDS only after the dissemination time (this happens the majority of the time). Note that the files outlined in yellow are the set of auxiliary files used during the reporting period.

Table 6.1-3: Table of historic GOM_PR2_AX files used by PDS for level 2 products generation. The GOM_PR2_AX is a file containing the configuration parameters used for processing from level 1b to level 2 products

Used by PDS for Level 2 products generation in period	GOM_PR2_AX (GOMOS Processing level 2 configuration file)
01-MAR-2002 → 29-JUL-2002	**GOM_PR2_AXVIEC20020121_165624_20020101_000000_20200101_000000** • Pre-launch configuration
30-JUL-2002 → 02-SEP-2002	**GOM_PR2_AXVIEC20020729_083851_20020301_000000_20100101_000000** • Maximum value of chi2 before a warning flag is raised (set to 5) • Maximum number of iterations for the main loop (set to 1)
03-SEP-2002 → 12-NOV-2003	**GOM_PR2_AXVIEC20020902_151029_20020301_000000_20100101_000000** • Maximum value of chi2 before a warning flag is raised (set to 100)
13-NOV-2003 → 22-MAR-2004	**GOM_PR2_AXVIEC20021112_170458_20020301_000000_20100101_000000** • Smoothing mode • Hanning filter • Number of iterations • Spectral windows to suppress the O2 absorption in the high spectral range of SPA2
23-MAR-2004 *Note*: this file was used by the GOMOS/4.02 processors before the IECF dissemination. The dissemination was done on 25th March 2004	**GOM_PR2_AXVIEC20040316_145613_20020301_000000_20100101_000000** • Pressure at the top of the atmosphere • Number of GOMOS sources data (used in GAP) • Activation flag for GOMOS sources data (GAP) • Smoothing mode (after the spectral inversion) • Atmosphere thickness

Table 6.1-4: Table of historic GOM_CRS_AX files used by PDS for level 2 products generation. The GOM_CRS_AX is a file containing the cross sections used for processing from level 1b to level 2 products

Used by PDS for Level 2 products generation in period	GOM_CRS_AX (GOMOS Cross Sections file)
01-MAR-2002 → 08-MAR-2002	**GOM_CRS_AXVIEC20020121_164026_20020101_000000_20200101_000000** • Pre-launch configuration
09-MAR-2003 → 29-JUL-2002	**GOM_CRS_AXVIEC20020308_185417_20020101_000000_20200101_000000** • Corrected NUM_DSD in MPH - was 14 and is now 19 - and corrected spare DSD format by replacing last spare by carriage returns in file GOM_CRS_AXVIEC20020121_164026_20020101_000000_20200101_000000

48

30-JUL-2002 → 25-MAR-2004	**GOM_CRS_AXVIEC20020729_082931_20020301_000000_20100101_000000** • O3 cross-sections summary description (SPA) • NO3 cross-sections summary description • O2 transmissions summary description • H2O transmissions summary description • O3 cross sections (SPA)
26-MAR-2004 _Note_: the file was disseminated on 27 Jan 2004 but could not be used by PDS until version GOMOS/4.02 was in operation	**GOM_CRS_AXVIEC20040127_150241_20020301_000000_20100101_000000** • Update of the O2 and H2O transmissions (S.A input) • Extension by continuity of the O3 cross-section for SPB

6.1.3 RE-PROCESSING STATUS

The improvement of the GOMOS processing chain is a continuous on-going activity, not only for the processing algorithm but also for the instrument characterization data. In order to provide the best quality products to the users and due to the normal delay between algorithm specification and implementation in the operational PDS, it has been decided to reprocess the GOMOS data using the GOPR prototype.

The first part of the second reprocessing activity covering years 2002-2005 and first three months of 2006 (using the prototype GOPR_6.0c_6.0f) is completed. Remaining gaps will be filled in 2006. All reprocessed data can be retrieved via web query from http://www.enviport.org/gomos/index.jsp. FTP access to bulk reprocessing results (one tar file of GOMOS products per day) is allowed from the D-PAC: ftp://gomo2usr@ftp-ops.de.envisat.esa.int.   See   more   details   and   latest   status   on http://www.enviport.org/boards/board_gomos.htm

6.2   Quality Flags Monitoring

In   this   section,   some   information   contained   in   the   Quality   Summary   data   set   of the level 2 products of June 2006 is shown. In particular, the percentage of flagged points per profile for the local species O_3, H_2O, NO_2 and Air is depicted. Only products in dark limb illumination conditions and without fatal errors (error flag in the MPH set to "0") are used.

A profile point in a level 2 product is flagged when:

- The local density is less than a given minimum value
- The local density is greater than a given maximum value
- A negative local density was found
- The line density is not valid. And it occurs when:
    - The acquisition from level 1b is not valid
    - There is no acquisition used for reference star spectrum
    - The line density is less than a given minimum value
    - The line density is greater than a given maximum value
    - A negative line density was found

49

For species: air, aerosol, O_3, NO_2, NO_3, OClO
- o   No convergence after a given number of LMA iterations
- o χ^2 out of LMA is bigger than χ^2
- o   Failure of inversion

For species: O_2, H_2O
- o   Spectro B only: no convergence
- o   Spectro B only: data not available
- o   Spectro B only: covariance not available

There are points mainly between -70° and +15° latitude because in this period of the year full dark illumination condition occultations (only those products have been used for these plots) are geo-located on that region. In summer, full dark illumination data are mainly in the Southern Hemisphere while in winter it is the contrary: full dark illumination occultations are found mainly in the Northern Hemisphere.

Looking at fig. 6.2-1, the most evident characteristic that can be observed is the high percentage of flagged points per profile for H_2O. Users should not use these data, as their quality is still poor. The percentage of flagged points per profile for O_3 and Air is around 35% whereas for NO_2 it becomes 60%. It can be seen also that there are latitudinal bands with almost the same color (same percentages). This means that the percentages of flagged points per profile have a dependence on the stars that have been observed: a given star is always observed at the same latitude but at different longitude.
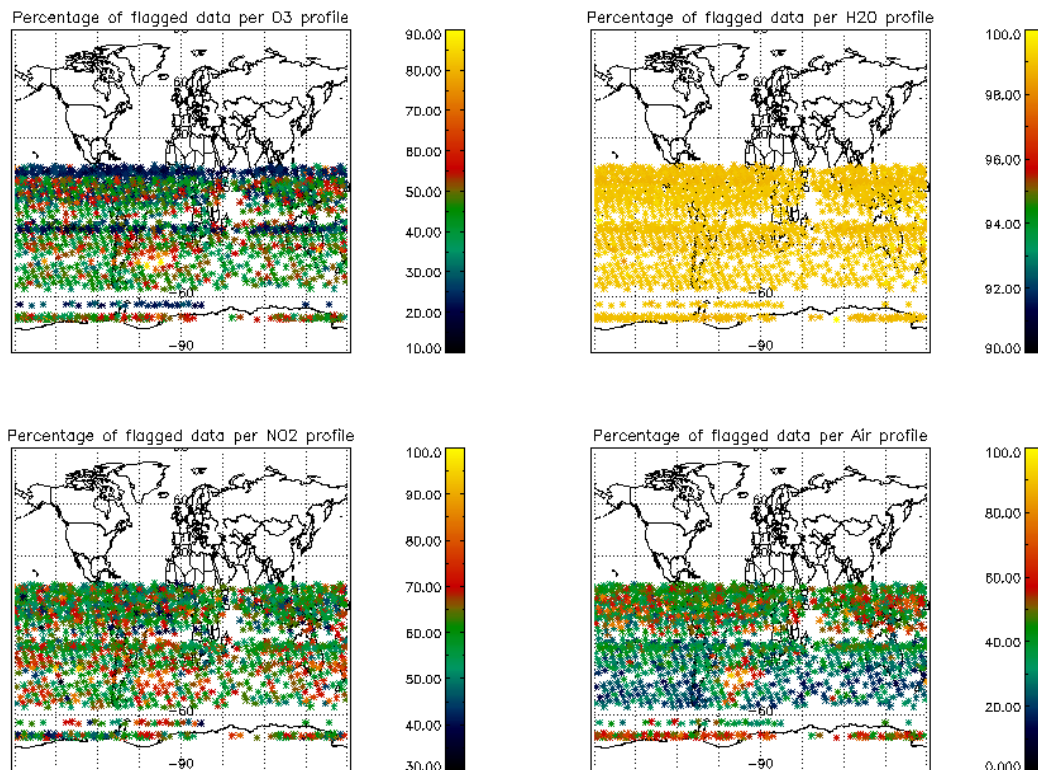

Figure 6.2-1: Percentage of flagged points per profile

Fig. 6.2-2 shows the same information as in fig. 6.2-1 but for given species **valid altitude ranges** (see table 6.2-1), that is, altitude ranges where data with the best quality should be found. If there are no points within the altitude range for a given occultation then a value of -20 is used. For O_3 the percentage of flagged points per profile is on average around 10% between 20 and 60 Km altitude. For NO_2 it becomes 30 % for altitudes between 20 and 50 Km and for Air profiles, the percentage of flagged points is around 15% for altitudes between 25 and 45 Km. For H_2O, considering the whole profiles or considering points below 50 Km does not change the high percentage of flagged points.

Table 6.2-1: Species valid altitude ranges

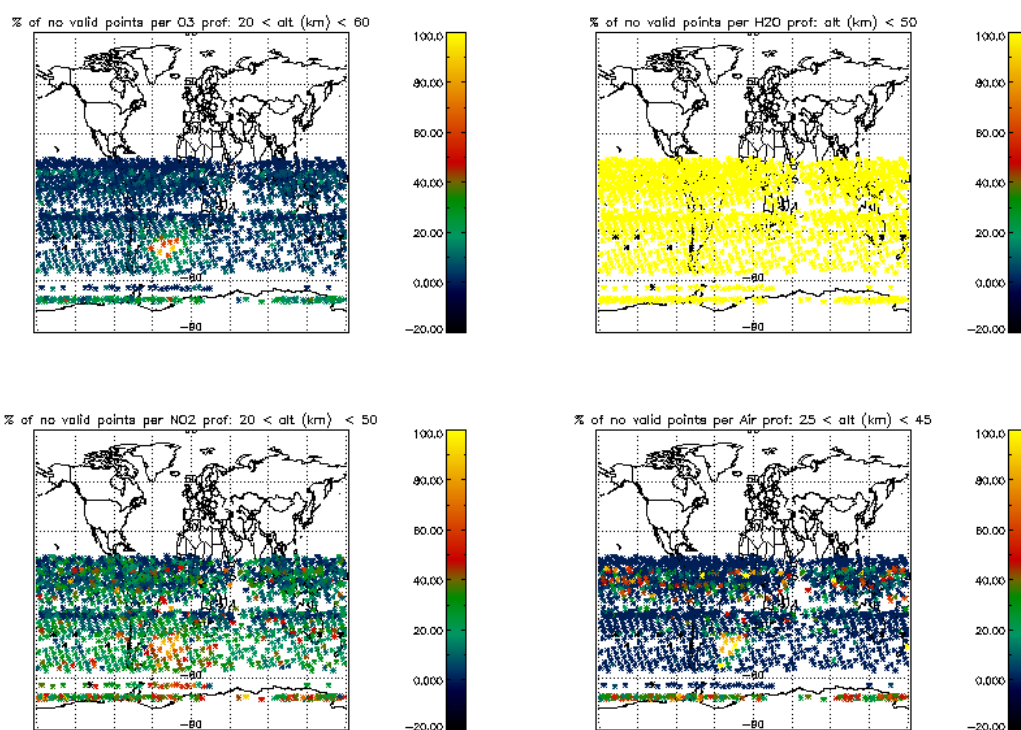| Specie	O_3	NO_2	Air	H_2O
Valid altitude range (km)	20 - 60	20 - 50	25 - 45	< 50

Figure 6.2-2: Same as fig. 6.2-1 but for valid altitude ranges of table 6.2-1

6.3 Other Level 2 Performance Issues

The plot presented in fig. 6.3-1 is the average of the Ozone values during June 2006 in a grid of 0.5 degrees in latitude per 1 km in altitude. Only occultations in dark limb have been used. Even though there is a reduction on latitude coverage due to the restricted azimuth field of view of the instrument, still some known characteristics can be seen:

- O_3 concentrations show a decrease with latitude near 40 km altitude. In the lower latitudes O_3 is generated by photolysis of O_2
- In the middle stratosphere (25-30 km) O_3 is strongly influenced by transport effects. Strong meridional and zonal transport is visible in middle and higher latitudes
- The lower stratosphere shows an O_3 increase with latitude. Highest values can be found within higher latitude regions due to downward transport of rich air masses

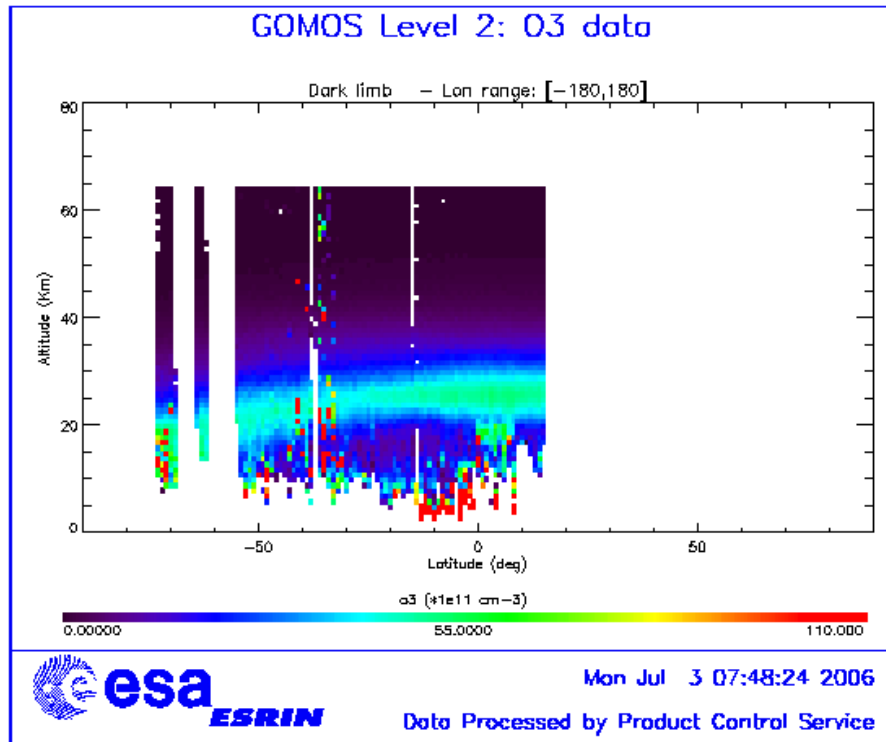For this month some problems can be seen at -30/-40 degrees latitudes, probably related with the SAA zone.

Figure 6.3-1: Average GOMOS O_3 profile during the reporting month: average in a grid of 0.5° latitude x 1 km altitude

7 VALIDATION ACTIVITIES AND RESULTS

7.1 *GOMOS-ECMWF Comparisons*

7.1.1 TEMPERATURE AND OZONE COMPARISONS

Due to restrictions in the current METEO product format, filtering of METEO data is not possible. ECMWF results are therefore partially based on data that are not to be used for scientific application, as mentioned in the disclaimer (http://envisat.esa.int/dataproducts/availability/disclaimers)

Find below the summary of ECMWF GOMOS monthly report for June 2006 data:

- The quality of GOMOS temperature and ozone data was found generally stable during June 2006, and comparable with that of May.
- Good agreement was found between GOMOS and ECMWF temperatures.
- GOMOS temperatures were lower than ECMWF temperatures in most of the stratosphere and mesosphere.
- The mean departures between GOMOS temperatures and ECMWF temperatures were less than -1% (about -2K) in the entire stratosphere, up to 1hPa. Negative departures down to -2% (about -4K) were found, on global average, in the mesosphere.
- The global mean departures between GOMOS and ECMWF ozone profiles were still found very large, with +50% differences in places, especially in the upper stratosphere and mesosphere.
- Large scatter of GOMOS ozone data was found at all latitudes.
- Scatter plots showed unrealistically low GOMOS ozone values (0 DU) at most vertical levels.
- No water vapour data were available in NRT GOMOS BUFR files.
- The monitoring statistics for June were produced with the operational ECMWF model, CY30R1.

The full June 2006 ECMWF report can be found in the link below:
http://earth.esa.int/pcs/envisat/tmp_calval_res/2006/ecmwf_gomos_monthly_200606_all.pdf

7.2 *GOMOS-Climatology comparisons*

Results are presented when available.

7.3 *GOMOS Assimilation*

Results are presented when available.

7.4 *Consistency Verification: GOMOS-GOMOS Inter-comparison*

7.4.1 QUALITY OF GOMOS O3 PROFILING IN BRIGHT LIMB

For an overall characterization of the quality of GOMOS day-time ozone profiles, bright-limb occultations of the very bright star S005 in January-February 2004 collocated with dark-limb occultations of "typical" star S025 were selected. These occultations are also relatively close in time and space to HALOE measurements. Information about these occultations is presented in table 7.4-1, and the location of GOMOS and HALOE profiles is shown in fig. 7.4-1. No strict collocation criteria were applied, as we are interested in mean values for climatology studies.

Table 7.4-1: GOMOS occultations in dark and bright limb selected for the analysis

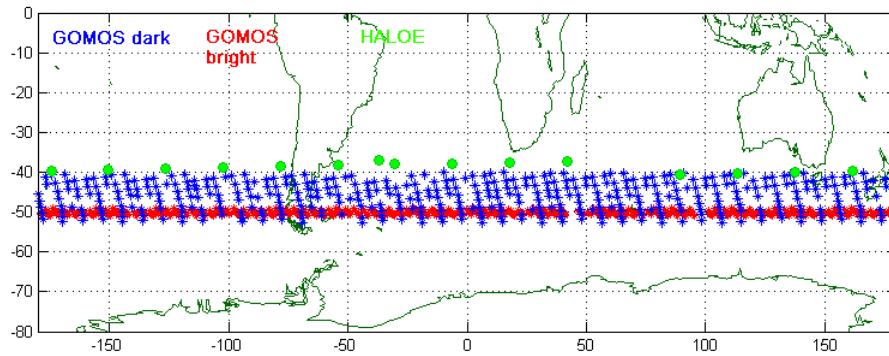|	*star*	*obliquity*	*number of occultations*
Bright	S005 (mv=0, T=11000K)	[-20;50]°	478
Dark	S025 (mv=1.6, T=28000K)	[5;45]°	428

Figure 7.4-1: Location of occultations (Jan-Feb 2004) selected for the comparison

We compared GOMOS bright limb and dark limb ozone profiles in the stratosphere (below 40 km), as it is known that ozone in the stratosphere is not subjected to diurnal variations at these altitudes. It is found that bright limb ozone profiles look unrealistic below ~33 km (fig. 7.4-2 and 7.4-3). In the upper stratosphere, the bright limb ozone profiles look realistic and have small variability. In the mesosphere and in the lower thermosphere (MLT), the diurnal variations of ozone are significant; therefore dark and night time ozone profiles cannot be directly compared at these altitudes. Qualitatively, we can expect always larger ozone concentrations in dark limb than in bright limb in MLT. This is observed at most altitudes in MLT, except at altitudes close to the ozone minimum (~80 km), where the median of day-time ozone concentrations exceeds that of night-time (fig. 7.4-3).
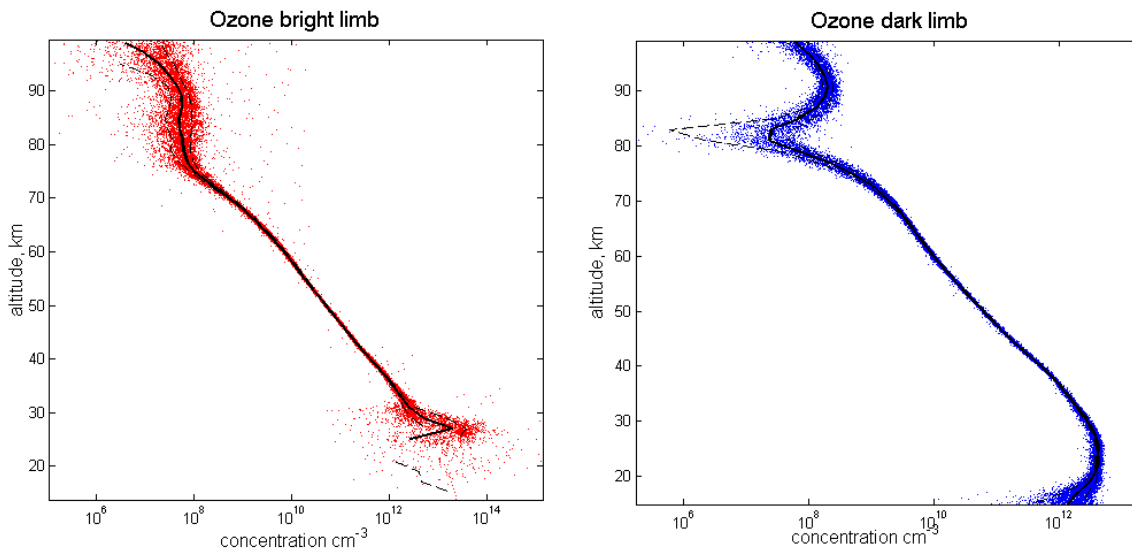

Figure 7.4-2: Comparison of collocated GOMOS dark and bright limb occultations: all profiles
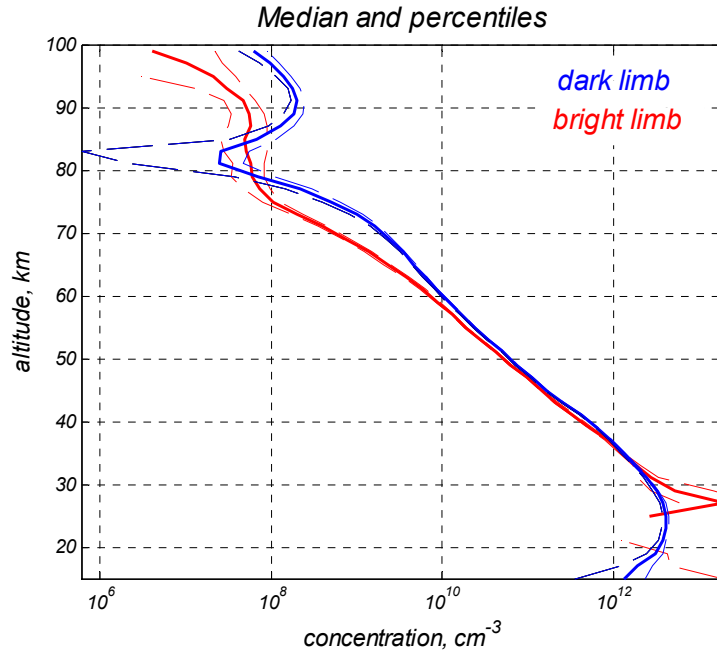
54

Figure 7.4-3: Comparison of collocated GOMOS dark and bright limb occultations: median profiles and percentiles (16th and 84th)

7.5 Inter-Comparison with external data

7.5.1 QUALITY OF GOMOS O3 PROFILING IN BRIGHT LIMB

The comparison between the median profiles of the two instruments shows that they are in relatively good agreement between 35km and 65km (zoom in fig. 7.5-1). As for the comparison with the full dark profiles, there is a large discrepancy between GOMOS and HALOE mean profiles close to the ozone minimum, with HALOE median profile lower than GOMOS bright-limb median profile around 80km.

As a preliminary conclusion, the day-time ozone profiles look realistic in the upper stratosphere and in the lower mesosphere, for bright stars. Extensive geophysical validation is needed to characterize quantitatively the accuracy of bright-limb GOMOS ozone profiling at these altitudes.
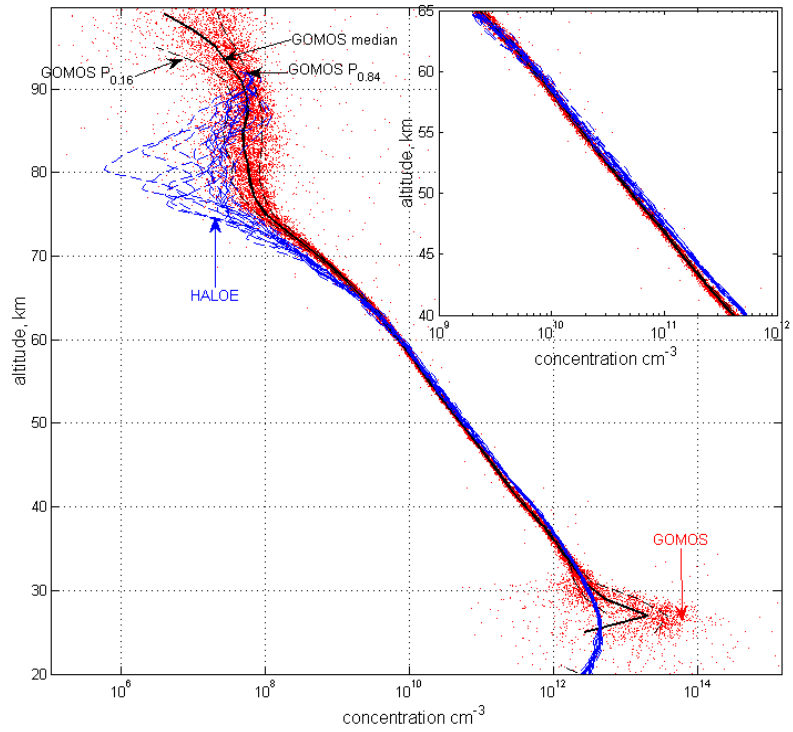
Figure 7.5-1: Comparison of GOMOS and HALOE data